Applications of Adjoint Error Correction for Integral Outputs

I. Michael Navon
School of Computational Science and Information Technology
Florida State University
Tallahassee, Florida 32306

Lecture Plan

- An introduction to adjoint error correction for integral outputs
- Linear adjoint error correction
- Nonlinear adjoint error correction
- Simple example
- Applications:
- Work with A.K. Alekseev, Department of Aerodynamics and Heat Transfer, RSC, ENERGIA, Korolev, Moscow Region 141070, Russian Federation.
  - A posteriori pointwise error estimation for Compressible fluid flows using adjoint parameters and Lagrange remainder Aleksey Alekseev and I M. Navon, International Journal for Numerical Methods in Fluids, 47, No. 1, 45-74 (2005)
  - Adjoint Correction and Bounding of Error Using Lagrange Form of Truncation Term. Aleksey K Alekseev and I.M. Navon, Computers & Mathematics with Applications, 50, 1311-1332 (2005)

- On a-posteriori pointwise error estimation using adjoint temperature and Lagrange remainder. Aleksey Alekseev and I M. Navon Computer Methods in Applied Mechanics and Engineering, 194/18-20, 2211-2228 (2005)
- A-Posteriori Error Estimation by Postprocessor Independent of Flowfield Calculation Method. Aleksey K Alekseev and I.M. Navon, Accepted for publication in Computers & Mathematics with Applications (2005)

- Work with
  C.C. Pain (Director), M.D. Piggott, G.C. Norman, F. Fang, D. P .Marshall, A.J. H. Goddard, Philip Power, Applied Modelling and Computational Group, Department of Earth Science and Engineering, Imperial College, London, UK.
  - Adjoint or goal-based error norms for adaptive mesh ocean modelling. P.W. Power and I.M. Navon To appear in Ocean Modelling.

  - Adjoint a-posteriori measures for anisotropic mesh optimization. P.W. Power, C.C. Pain, M.D. Piggott, F. Fang, G.J. Gorman, A.P. Umpelby, A.J.H. Goddard and I.M. Navon Accepted for publication in Computers & Mathematics with Applications (2005)
  - Ph.D. Thesis of: Philip William Power, BSc, ARCS: ERROR MEASURES FOR FINITE ELEMENT OCEAN MODELLING (2005).

- Efficient model reduction using POD- KL and combined with goal oriented (dual- weighted residual) methods.
- Future work and Conclusions

Introduction

Motivation

Aerodynamics

- Interest in integral outputs- also referred to as output functionals arises in many applications in CFD.
- Infrared signature of tanks or aircrafts (volume integrals).
- Lift and drag in aerodynamics (surface integrals).

The goal-oriented methods are concerned with analysis of error in these functionals and with a particular method that greatly reduces the error in many cases doubling order of accuracy for the functional compared to relative underlying flow solution.

This is very different from other approaches that focus on

- maximum
- root mean square
- measures of error in the entire flow field

Grid refinement for computed lift or drag (serving as chosen output functionals) related to wake behind a wing is related to local refinement near leading and trailing edge where small errors have large impact on the lift or drag.

Adjoint error correction and a-posteriori error analysis

A priori error estimates are typically representing error bound, error $< c\,h^p$,

where h is grid spacing, c and p are positive constants independent of h. p measures how rapidly error reduces as we refine discretization mesh.

On structured grids error is proportional to truncation error.

c depends on other factor such as

- geometry of computational domain
- boundary conditions

Very difficult to evaluate c.

A-posteriori error analysis

$$error < e(u_h)$$

We wish to have a guaranteed error bound, where $e(u_h)$ is a computable function of numerical solution u_h.

This provides us with knowledge that true value of integral output is within certain limits (bounds).

Such bounds have to be tight i.e,

$$1 \leqslant \frac{e(u_h)}{error} \leqslant 10$$

However nonlinearities stand in the way and usually a-posteriori error bounds are asymptotic,

$$error < e(u_h), \forall h < h_0.$$

Problem: value of h_0 is not known.

Distinction between guaranteed and asymptotic bounds since with asymptotic bound- we must exercise judgment about mesh resolution to find out if bound is valid.

With guaranteed bound we can start with coarse mesh and refine which numerical solution satisfies pre-set tolerance.

Error bounds based on adjoint solution require similar effort to adjoint error correction.

Knowing estimate of this error can be used to correct leading order terms in error i.e, obtain a solution with higher order of accuracy.

Use of adjoints for error analysis of output (goal) functionals: Algebraic framework

Consider $\mathbf{g}^T\,\mathbf{u}$ (scalar product)

u-solution of system of linear equations,

$$A\,\mathbf{u} = \mathbf{f}.$$

Dual (adjoint) treatment consists in evaluating $\mathbf{v}^T\,\mathbf{f}$ where $\mathbf{v}$ is solution of adjoint (dual) equations,

$$A^T\,\mathbf{v} = \mathbf{g}.$$

The two calculations are equivalent due to the following identity,

$$\mathbf{v}^T(A\mathbf{u}) = (A^T\mathbf{v})^T\,\mathbf{u},$$

from which we derive,

$$\mathbf{v}^T\mathbf{f} = \mathbf{g}^T\mathbf{u}.$$

To obtain linear output functional from solution of linear system of equations

- One can either solve primal system of equations
- Solve adjoint (dual system of equations)

For differential equations the vector product corresponds to integral inner product and $\mathbf{A}^T$ corresponds to adjoint differential operator.

The adjoint identity above also includes certain boundary integral terms.

When output is required for a single f or g there is no advantage in using the adjoint approach.

The same computational cost is required for either primal or dual.

When value of the output is wanted for a single g but for different vectors f - the direct approach requires solution of the primal equations for each value of f.

While the dual approach only requires one adjoint calculation followed by an inexpensive vector product

$$\mathbf{v}^T\mathbf{f}$$

for each $\mathbf{f}$.

The Adjoint approach in numerical analysis and engineering design

- This result can be used in two different contexts :
- Design optimization (see Anthony Jameson 1995, Alexandrov et al. , 1997)
- Anderson and Venkatakrishnan :Aerodynamic Design Optimization 1999.
- Error analysis

The design optimization provided "industrial"pay-off.

Error analysis is less appreciated but is attracting now many researchers.

Consider system with $\mathbf{U}$ vector flow-variables at discrete set of points with coordinates, X, solution of system of nonlinear equations

$$N(X, \mathbf{U}),$$

arising from either Euler or Navier-Stokes equations plus boundary conditions.

Via grid generation process- grid coordinates depend on α representing one or more geometric design variables. For one design variable α we linearize about flow solution for baseline geometry to get

$$A\mathbf{u} = \mathbf{f},$$

where $\mathbf{u}$ is the sensitivity of flow field to changes in α,

$$\mathbf{u} = \frac{\partial \mathbf{U}}{\partial \alpha},$$

$$A = \frac{\partial N}{\partial \mathbf{U}},$$

$$\mathbf{f} = -\frac{\partial N}{\partial X}\frac{\partial X}{\partial \alpha}.$$

Target of design optimization is minimizing some objective function

$$J(\mathbf{U}, \mathbf{X})$$

(For example discrete approximation to drag)

Linearizing objective function yields

$$\frac{\partial J}{\partial \alpha} = \mathbf{g}^T \mathbf{u} + \frac{\partial J}{\partial \mathbf{X}} \frac{\partial \mathbf{X}}{\partial \alpha}$$

$$\mathbf{g}^T = \frac{\partial J}{\partial \mathbf{U}}$$

In adjoint method, the sensitivity of objective function to changes in α is obtained from

$$\frac{\partial J}{\partial \alpha} = \mathbf{v}^T \mathbf{f} + \frac{\partial J}{\partial \mathbf{X}} \frac{\partial \mathbf{X}}{\partial \alpha}$$

with $\mathbf{v}$ satisfying adjoint equations.

$$\mathbf{A}^T\mathbf{v} = \mathbf{g}$$

If there are several design variables, each has different $\mathbf{f}$ but same $\mathbf{g}$ so calculation via adjoint approach is much cheaper, requiring solution of only one adjoint set of equations.

Error analysis

Let us consider again evaluating $g^T\ \mathbf{u}$ with $\mathbf{u}$ being solution of system of linear equations.

$$\mathbf{A}\mathbf{u}\ =\ \mathbf{f}$$

The corresponding dual(adjoint) is to evaluate $\mathbf{v}^T\ \mathbf{f}$ where $\mathbf{v}$ is solution of the adjoint equations:

$$\mathbf{A}^T\mathbf{v}\ =\ \mathbf{g}$$

If we have approximate solutions $\tilde{\mathbf{u}}$, $\tilde{\mathbf{v}}$ to each of these equations we obtain

$$\begin{aligned}
\mathbf{g}^T\,\mathbf{u} &= \mathbf{g}^T\,\tilde{\mathbf{u}} + \mathbf{g}^T\,(\mathbf{u}-\tilde{\mathbf{u}}) \\
&= \mathbf{g}^T\,\tilde{\mathbf{u}} + \mathbf{v}^T\,\mathbf{A}\,(\mathbf{u}-\tilde{\mathbf{u}}) \\
&= \mathbf{g}^T\,\tilde{\mathbf{u}} + \mathbf{v}^T\,\mathbf{A}\,(\mathbf{u}-\tilde{\mathbf{u}}) + (\mathbf{v}-\tilde{\mathbf{v}})\,\mathbf{A}\,(\mathbf{u}-\tilde{\mathbf{u}}) \\
&= \underbrace{\mathbf{g}^T\tilde{\mathbf{u}}}_{I} + \underbrace{\mathbf{v}^T\,(\mathbf{A}\,\tilde{\mathbf{u}} - \mathbf{f})}_{II} + \underbrace{(\mathbf{v}-\tilde{\mathbf{v}})\,\mathbf{A}\,(\mathbf{u}-\tilde{\mathbf{u}})}_{III}
\end{aligned} \tag{1}$$

(I) is the value of functional using approximate solution $\tilde{\mathbf{u}}$

(II) is computable since it involves known approximate solutions $\tilde{\mathbf{u}}$ and $\tilde{\mathbf{v}}$

Third term is not computable if exact solutions $\mathbf{u}$ and $\mathbf{v}$ are not known.

If $\tilde{\mathbf{u}}$ and $\tilde{\mathbf{v}}$ are close approximations to $\mathbf{u}$ and $\mathbf{v}$ then third term is very small.

Sum of first two terms is good approximation to true value of $\mathbf{g}^T\mathbf{u}$.-a much better approximation than $\mathbf{g}^T\tilde{\mathbf{u}}$

The second term is referred to as the adjoint error correction term. $\mathbf{A}\tilde{\mathbf{u}} = \mathbf{f}$ is residual error in solving the system $\mathbf{A}\tilde{\mathbf{u}} = \mathbf{f}$.

The approximate adjoint solution $\tilde{\mathbf{v}}$ provides weighting for residual error, providing for effect of residual error on output functional of interest.

This inner product of a residual error and an adjoint weighting is of interest.

To evaluate nonlinear function $J(\mathbf{U})$. $\mathbf{U}$ satisfying solution of nonlinear equations.

$$N(\mathbf{U}) \;=\; 0$$

Given an approximate solution $\tilde{\mathbf{U}}$ we define as solution error

$$\mathbf{u} = \tilde{\mathbf{U}} - \mathbf{U}$$

Let us linearize both nonlinear equations and functional

$$N(\tilde{\mathbf{U}}) \;=\; N(\mathbf{U}+\mathbf{u}) \;\approx\; \frac{\partial N}{\partial \mathbf{U}}\;\mathbf{u}$$

$$J(\tilde{\mathbf{U}}) \;=\; J(\mathbf{U}+\mathbf{u}) \;\approx\; J(\mathbf{U})\;\frac{\partial J}{\partial \mathbf{U}}\;\mathbf{u}$$

We can write these as

$$\mathbf{A}\mathbf{u} = f,$$

$$\mathbf{A} = \frac{\partial N}{\partial U}, \mathbf{f} = N(\tilde{\mathbf{U}}),$$

$$J(\mathbf{U}) \approx J(\tilde{\mathbf{U}}) - \mathbf{g}^T \mathbf{u},$$

where

$$\mathbf{g}^T = \frac{\partial \mathbf{T}}{\partial \mathbf{U}}.$$

Let $\mathbf{v}$ be defined as satisfying adjoint equation $\mathbf{A}^T\mathbf{v} = \mathbf{g}$

we obtain

$$J(\tilde{\mathbf{U}}) = J(\tilde{\mathbf{U}}) - \mathbf{v}^T\mathbf{f} = J(\tilde{\mathbf{U}}) - \tilde{\mathbf{v}}^T N(\tilde{\mathbf{U}})$$

The quantity $J(\tilde{\mathbf{U}}) - \tilde{\mathbf{v}}^T N(\tilde{\mathbf{U}})$ provides a more accurate estimate for $J(\mathbf{U})$ then $J(\tilde{\mathbf{U}})$ alone.

Adjoint error correction term = product of an approximate adjoint solution and the residual error from the nonlinear equations.

History of use of adjoints for error analysis

1967- Aubin and Nitsche who used adjoint to derive a priori optimal order proofs of L_2 convergence of finite element methods for elliptic pdes.

1978 - Babuska and Rheinboldt developed 'a posteriori' error analysis applied to Poisson and Cauchy Riemann equations.

1984 Babuska and Miller focused attention on integral functional outputs.

1987 Barrett and Elliott analyze problem in convection diffusion for non-self adjoint problems making a vital connection to CFD problems.

Late 1990- explosion in research in 'a-posteriori' adjoint error correction (see Suli, Johnson, Ranacher and Becker to cite but a few) used finite element method a posteriori error bounds to derive good grid adaption indicators.

Giles and Piece. Extended adjoint correction ideas to finite volume methods and the the superconvergence concept that is natural for finite element methods.

Venditti and Darmofal (2000, 2001) used an algebraic version of the adjoint error correction and used it to derive grid mesh refinement adaptation criteria.

Brief outline of adjoint error correction

Let $\mathbf{u}$ be solution of a linear differential equation

$$\mathbf{Lu} = \mathbf{f}$$

on a domain Ω subject to homogeneous b.c's for which problem is well posed when

$$\mathbf{f} \in \mathbf{L}_2(\Omega)$$

i.e $\mathbf{f}$ is a square integrable function. The adjoint differential operator L^* and associated homogeneous b.c. are defined by the identity

$$(\mathbf{v}, \mathbf{Lu}) \;=\; (\mathbf{L}^*\mathbf{v}, \mathbf{u})$$

that holds for all $\mathbf{u}$ and $\mathbf{v}$ satisfying the boundary conditions.

The (,) stands for integral inner product over domain Ω

$$(\mathbf{v}, \mathbf{Lu}) \;=\; \int_\Omega \mathbf{v^T}\,\mathbf{Lu}\,\mathbf{dV}$$

$\mathbf{u}$ and $\mathbf{v}$ may be vector functions.

Definition of L^* is obtained via integration by parts starting from $(\mathbf{v}, \mathbf{Lu})$ until all derivatives act on $\mathbf{v}$ rather than on $\mathbf{u}$.

The adjoint b.c's come from requiring that boundary terms arising from integration by parts be zero.

Consider value of functional

$$J = (\mathbf{g}, \mathbf{u}), \quad \mathbf{g} \in L_2(\Omega)$$

A dual formulation is to evaluate functional

$$J = (\mathbf{v}, \mathbf{f})$$

where $\mathbf{v}$ satisfies the adjoint equation

$$\mathbf{L}^*\mathbf{v} \;=\; \mathbf{g}$$

subject to homogeneous adjoint b.c.'s. We have

$$(\mathbf{v}, \mathbf{f}) \;=\; (\mathbf{v}, \mathbf{Lu}) \;=\; (\mathbf{L}^*\mathbf{v}, \mathbf{u}) \;=\; (\mathbf{g}, \mathbf{u})$$

Let $\mathbf{u}_h$ and $\mathbf{v}_h$ be numerical approximations to $\mathbf{u}$ and $\mathbf{v}$ respectively and satisfy the homogeneous boundary conditions.

Subscript h denotes that approximate solutions are obtained from numerical computation with a grid whose average spacing is h.

We assume $\mathbf{u}_h$ and $\mathbf{v}_h$ sufficiently smooth so that

$$\mathbf{L}\mathbf{u}_h,\ \mathbf{L}^*\mathbf{v}_h$$

lie in $L_2(\Omega)$

$$\mathbf{L}\mathbf{u}_h - \mathbf{f},$$

and

$$\mathbf{L}^*\mathbf{v}_h - \mathbf{h}$$

are residual errors whose magnitude measures extent to which $\mathbf{u}_h$ and $\mathbf{v}_h$ are not the true solutions.

We get

$$\begin{aligned}(g,u) &= (g,u_h) - (L^*v_h, u_h - u) + (L^*v_h - g, u_h - u) \qquad (2)\\ &= (g,u_h) - (v_h, L(u_h - u)) + (L^*(v_h - v), u_h - u)\\ &= \underbrace{(g,u_h)}_{I} - \underbrace{(v_h, Lu_h - f)}_{II} + (v_h - v, L(u_h - u))\end{aligned}$$

(I)- value of functional obtained using approximate solution u_h

(II)- inner product of residual error $L\,u_h - f$ and approximate adjoint solution v_h.

The adjoint solution provides weighting of local residual error to overall error in computed functional.

• Evaluating and subtracting this adjoint error allows obtaining a more accurate value of functional.

If

$$Lu_h = L(u_h - u) \sim u_h - u,$$

then remaining error has a bound proportional to product $\|u_h - u\| \, \|v_h - v\|$ (by using L_2- norm), so that corrected functional value is superconvergent.

If

$$u_h - u \sim O(h^p), v_h - v \sim O(h^p),$$

Then the error in the functional is $O(h^{2p})$.

Simple example

1-D Poisson equation.

$$\frac{d^2u}{dx^2} = f,\ x \in [0,1]$$

subject to homogeneous boundary conditions $u(0) = u(1) = 0$.

The dual is the Poisson equation,

$$\frac{d^2v}{dx^2} = g,$$

with the same homogeneous boundary conditions.

Adjoint identity verified (u and v equal to 0 at each end).

$$\int_0^1 v\frac{d^2u}{dx^2}dx = -\int_0^1 \frac{dv}{dx}\frac{du}{dx}dx = \int_0^1 \frac{d^2v}{dx^2}\,u\,dx$$

Poisson equation is numerically approximated on uniform grid, mesh size h

with 2-nd order finite difference (approximation) discretization,

$$h^{-2}\,\delta_x^2 u_j = \frac{u_{i+1} - 2u_i + u_{i+1}}{h^2} = f(u_j).$$

Approximate solution $u_h(x)$ is defined by cubic spline interpolation through model values x_f.

The adjoint solution v_h is obtained exactly in the same manner.

Numerical results plotted for case,

$$f(x) = x^3\,(1-x)^3,\ g = \sin(\pi\,x),$$

Fig. 1 shows residual error, $L\,u_h - f$ for $h = 1/32$ as well as the 3 Gaussian quadrature points on each subinterval that are useful in numerical integration of inner product $(v_h, L\,u_h - f)$, since u_h is a cubic spline, $f_h = \frac{d^2 u_h}{dx^2}$ is continuous piecewise linear.

The dominant term of approximation error is quadratic on each subinterval.

Adjoint solution v_h illustrates that residual error in center of domain contributes the most to overall error in functional.

Fig. 3 is log- log plot of 3 quantities vs number of mesh- cells:

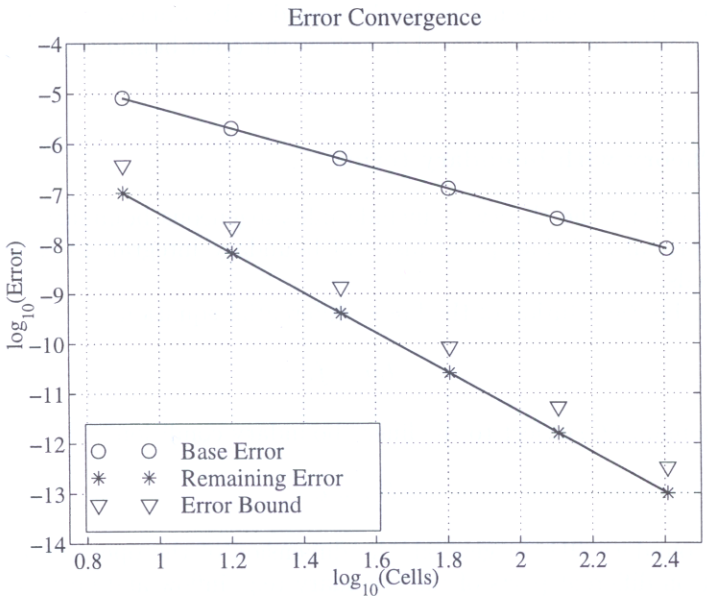

Fig. 3. Functional error convergence for 1D Poisson equation.

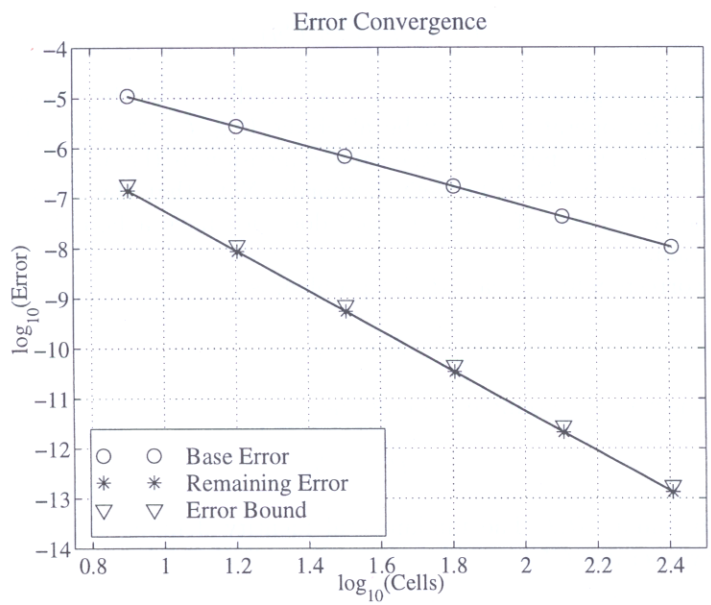

Fig. 4. Functional error convergence for 2D Poisson equation.

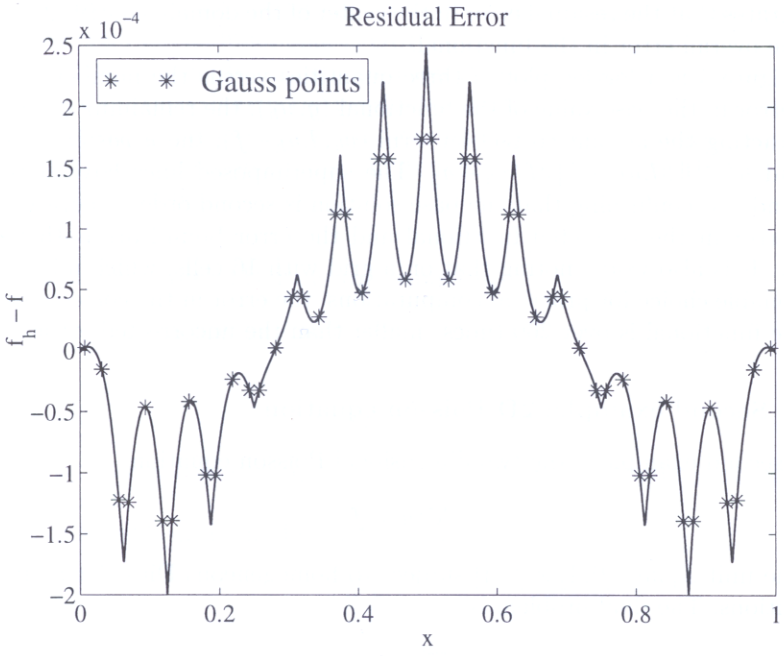

Fig. 1. Residual error for 1D Poisson equation.

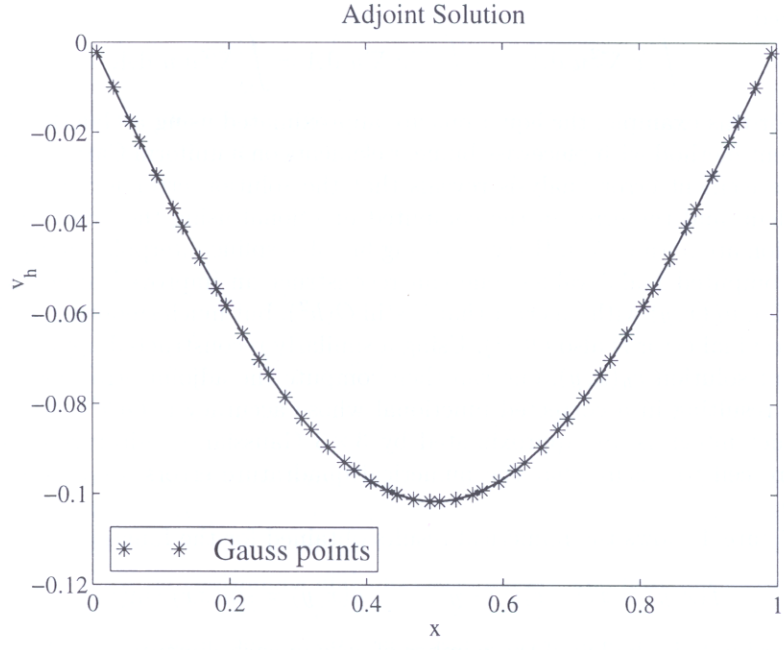

Fig. 2. Adjoint solution for 1D Poisson equation.

1. Error in base value of functional (g, u_h).
2. Remaining error after subtracting adjoint correction term, $(v_h, Lu_h - f)$.
3. The a-posteriori error bound,

$$\|L^{-1}\|\|Lu_h - f\|\|L^* v_h - g\|.$$

The superimposed lines have slopes of -2 and -4 confirming that base solution is $O(h^2)$ accurate while error in the corrected functional as well as error bound are both 4-th order.

For a 16 cell grid we note that the error in adjoint corrected value of functional is over 200 times smaller ($(1/h^2)$) than the uncorrected error.

Nonlinear adjoint error correction

We need to address issues in linearizing nonlinear functionals and operators.

If u is a scalar variable and $f(u)$ is a nonlinear scalar functional using Taylor series,

$$f(u_2) = f(u_1) + f'(u_1)(u_2 - u_1) + O((u_2 - u_1)^2).$$

We can also obtain exact expression without remainder by

$$\frac{\partial}{\partial\theta} f(u_1 + \theta(u_2 - u_1)) = f'(u_1 + \theta(u_2 - u_1))(u_2 - u_1),$$

Integrate it from $\theta = 0$ to $\theta = 1$,

$$f(u_2) - f(u_1) = \overline{f}'(u_1, u_2)(u_2 - u_1),$$

where $\overline{f}'(u_1, u_2) = \int_0^1 f'(u_1 + \theta(u_2 - u_1))d\theta$.

If $\mathbf{u}$ and $\mathbf{f}$ are vectors we need to define a Jacobian matrix,

$$A\mathbf{u} = [\frac{\partial f}{\partial u}]_u,$$

Subscript u denotes that value of Jacobian matrix A depends on value of $\mathbf{u}$ around which $f(\mathbf{u})$ is linearized.

We obtain

$$\frac{\partial}{\partial\theta} f(u_1 + \theta(u_2 - u_1)) = A_{u_1+\theta(u_2-u_1)}.$$

Integrating over θ yields,

$$f(u_2) - f(u_1) = \overline{A}_{(u_2,u_1)}(u_2 - u_1),$$

where

$$\overline{A}_{(u_1,u_2)} = \int_0^1 [\frac{\partial f}{\partial u}]_{u_1=\theta(u_2-u_1)} d\theta.$$

Next consider a nonlinear operator $N(u)$.

The linearized operator $L\,u$ is called a Fréchet derivative and is formally defined as,

$$L_u\,\widetilde{u} = lim_{\epsilon \to 0} \frac{N(u + \epsilon\widetilde{u}) - N(u)}{\epsilon},$$

Subscript u denotes fact that linear operator matrix depends on value of u around which $N(u)$ is linearized.

If $N(u)$ is nonlinear advection diffusion 1-D,

$$N(u) = \frac{\partial}{\partial x}(\frac{1}{2}u^2) - \nu\frac{\partial^2 u}{\partial x^2}$$

then

$$L_u\,\widetilde{u} = \frac{\partial}{\partial x}(u\widetilde{u}) - \nu\frac{\partial^2 \widetilde{u}}{\partial x^2}$$

In a final step one starts from

$$\frac{\partial}{\partial\theta}N(u_1+\theta(u_2-u_1))=L_{u_1+\theta(u_2-u_1)}(u_2-u_1)$$

Integrate over θ and obtain

$$N(u_2)-N(u_1)=\overline{L}_{u_1,u_2}(u_2-u_1)$$

$$\overline{L}_{u_1,u_2}=\int_0^1 L_{u_1+\theta(u_2-u_1)}d\theta$$

$\overline{L}_{u_1,u_2}$ is average value of the linear operator L_u over "path" from u_1 to u_2.

Grid-Adaptation based on a-posteriori error estimates

Provides for robust refinement criteria in practice.

1st. Approach

Consider dominant correction term in product

$$(v_h, N(u_h))$$

expressed as sum of contribution from each cell in the domain,

$$(v_h, N(u_h)) = \Sigma_\alpha (v_h, N(u_h))_\alpha .$$

First strategy is to subdivide all cells for which

$$(v_h, N(u_h))_\alpha > \epsilon_{tol} .$$

Purpose of adjoint correction in this application is questionable.

2 Estimated remaining error term

After making adjoint error correction the remaining error term can be expressed as

$$(v - v_h, N(u_h)).$$

However analytic *adjoint* solution v is not known.

An option is to attempt to estimate it and adapt those cells in which

$$(v - v_h, N(u_h))_\alpha > \epsilon_{tol}$$

How to estimate v ?

1. Becker and Ranacher (2001) use quadratic reconstruction to estimate v, having used a piecewise linear f.e.m. for r_h.

If one uses Galerkin f.e.m., due to orthogonality $(v - v_h, N(u_h))$ has some value for any v_h in appropriate finite element space.

Consider a different v_h, interpolant of v, so $v - v_h$ is interpolation error- which may be estimated using computed adjoint section.

- Venditti and Darmofal (2001) consider dominant part of remaining error

$$(R_h, u - u_h)$$

with $R_h \equiv L^*_{u_h} v_h - g(u_h)$ is the residual error is satisfying adjoint p.d.e.

They decide to adapt (i.e., subdivide) any cell in which

$$|(v - v_h), N(u_h)|_\alpha + |(R_h, u - u_h)|_\alpha > \epsilon_{threshold}.$$

The analytic solution u and v are again approximated by a high- order reconstruction.

Option 3: Coarse grid error estimates using residual error from both the original and adjoint (method) problem express dominant error as

$$|L^*_{u_h} R_h, N(u_h)| \approx (R_h, L^{-1}_{u_h} N(u_h))$$

Using this in adaptive approach has a problem since $L^{-1}_{u_h}$ is a global operator.

Solution: Use coarse mesh to approximately evaluate $L^{-1}_{u_h} N(u_h)$ and $L^{*-1}_{u_h} N(u_h) R_h$ and then adapt in any cell α for which

$$|L^{*-1}_{u_h} R_h, N(u_h))|_\alpha + |(R_h, L^{-1}_{u_h} N(u_h))_\alpha| > \epsilon_{tol}.$$

A choice is made between improved accuracy or a tight bound.

A-posteriori pointwise error estimation using adjoint temperature and Lagrange remainder

- Use local truncation error estimated from Taylor series with remainder in Lagrange form.
- The adjoint equations are in a continuous form.

We consider temperature error at a verification point for a finite-difference discretization of time dependent 1-D heat equation.

$$c\rho\frac{\partial\widetilde{T}}{\partial t} - \frac{\partial}{\partial x}(\lambda\frac{\partial\widetilde{T}}{\partial x}) = 0$$

in $\Omega \times (0, t_f)$, where $\Omega \in \Re^1$.

with initial conditions,

$$\widetilde{T}(0, x) = T_0(x),$$

where $T_0(x) \in L_2(\Gamma_i)$,

b.c' s

$$\frac{\partial\widetilde{T}}{\partial x}|_{x=0} = 0,$$

and

$$\frac{\partial \widetilde{T}}{\partial x}|_{x=\chi} = 0,$$

where c is thermal capacity,

λ is thermal conductivity,

ρ is density,

$\widetilde{T}$ is exact, nonperturbed temperature,

χ is thickness,

t is time,

t_f is final time (duration of process),

ρ, c are constants.

2 CASES CONSIDERED

1. $\lambda =$ constant, $\widetilde{T}(t,x) \in C^{\infty}(Q)$,
2. $\lambda \in L_2(\Omega)$, $\widetilde{T}(t,x) \in H^1(Q)$.

Consider a finite difference approximation (first order in time, second order in space),

$$c\rho\frac{T_k^n - T_k^{n-1}}{\Delta t} - \lambda\frac{T_{k+1}^n - 2T_k^n + T_{k-1}^n}{h_k^2} = 0 \tag{3}$$

If we expand mesh-function T_k^n in a Taylor series and substitute to Eq. (3), then we obtain the following differential approximation,

$$c\rho\frac{\partial T}{\partial t} - \lambda\frac{\partial^2 T}{\partial x^2} + \delta T = 0, \tag{4}$$

$$\begin{aligned} \delta T_t &= -\frac{c\rho}{2}\tau\frac{\partial^2 T(t_n - \alpha_k^n\tau, x_k)}{\partial t^2}, \qquad (5)\\ \delta T_x &= -\frac{\lambda}{24}h_k^2\left(\frac{\partial^4 T(t_n, x_k + \beta_k^n h)}{\partial x^4} + \frac{\partial^4 T(t_n, x_k - \gamma_k^n h)}{\partial x^4}\right) \end{aligned}$$

We use here $\delta T = \delta T_t + \delta T_x$ and the Lagrange form of the remainder with unknown parameters $\alpha_k^n, \beta_k^n, \gamma_k^n \in (0,1)$.

By introducing solution error $\Delta T (T = \widetilde{T} + \Delta T)$.

We reformulate Eq.(4) as

$$c\rho \frac{\partial(\widetilde{T} + \Delta T)}{\partial t} - \lambda \frac{\partial^2(\widetilde{T} + \Delta T)}{\partial x^2} + \delta T = 0. \tag{6}$$

We address impact of distributing source terms on temperature at a checkpoint.

Error of temperature calculation at checkpoint $T(t_{est}, x_{est})$ determined by sum of contributions of LTE with weights depending on transfer of disturbances.

Denote T_{est} by $\mathcal{J}$ and express it as a functional,

$$\mathcal{J} = \int \int_{\Omega} T(x,t)\delta(t - t_{est})\delta(x - x_{est}) dt\, dx, \tag{7}$$

where δ is the Dirac delta function.

We introduce a Lagrangian comprised of estimated value and weak statement

of Eq. (7),

$$
\begin{aligned}
L &= \int\int_{\Omega} T(x,t)\delta(t-t_{est})\delta(x-x_{est})dt\,dx \qquad (8)\\
&+ \int\int_{\Omega} c\rho\frac{\partial T}{\partial t}\Psi(x,t)dt\,dx\\
&- \int\int_{\Omega} \frac{\partial}{\partial x}(\lambda\frac{\partial T}{\partial x})\Psi(x,t)dt\,dx + \int\int_{\Omega}\delta T\Psi dt\,dx.
\end{aligned}
$$

Here Ψ is adjoint temperature.

Calculating variation of Lagrangian and use of integration by parts, we can express variation of Lagrangian via disturbing term δT as,

$$\Delta L = \int \int_{\Omega} \delta T \Psi(x,t) dt\, dx \tag{9}$$

We end up looking for solution of the following adjoint (dual) problem,

$$c\rho \frac{\partial \Psi}{\partial t} + \frac{\partial}{\partial x}(\lambda \frac{\partial \Psi}{\partial x}) - \delta(t - t_{est})\delta(x - x_{est}) = 0, \;\; (x,t) \in \Omega, \tag{10}$$

with boundary conditions,

$$\frac{\partial \Psi}{\partial x}|_{x=\chi} \; = 0, \quad \frac{\partial \Psi}{\partial x}|_{x=0} \; = 0, \tag{11}$$

and initial condition,

$$\Psi(x, t_f) = 0. \tag{12}$$

Analytic solution of the adjoint temperature equation, (10), corresponds to a Green' s function of the heat transfer equation,

$$\Psi(x,t) = \frac{Q}{2\sqrt{\frac{\pi\lambda}{C\rho}(t_{est} - t)}} \exp\left(\frac{-(x - x_{est})^2}{4\lambda/(C\rho)(t_{est} - t)}\right) \tag{13}$$

It is known that

$$\Delta\mathcal{J}(\delta T) = \Delta L(\delta T, \Psi),$$

for the solution of direct and adjoint problems.

Thus we determine variation of $T(x_{est}, t_{est})$ as,

$$\Delta T_{est} = T_{est} - T_{exact} = \int\int_{\Omega} \delta T \Psi_{exact}(x,t) dt\, dx \tag{14}$$

Adjoint temperature allows us to calculate variation of estimated parameter as a function of the truncation error.

The error of temperature for verification point is divided into 2 parts,

$$\Delta T_{est} = \int\int_{\Omega} \delta T \Psi_{exact}(x,t) dt\, dx + \int\int_{\Omega} \delta T \Delta\Psi(x,t) dt\, dx \qquad (15)$$

Estimation of error due to time approximation,

$$\frac{C\rho}{2} \sum_{k=1,\, n=2}^{N_x\ N_t} \alpha_k^n \tau^3 \frac{\partial^3 T(t_n, x_k)}{\partial t^3} \Psi_k^n h_k \quad \leq$$

$$\frac{C\rho}{2} \sum_{k=1,\, n=2}^{N_x\ N_t} |h_k \tau^3 \frac{\partial^3 T(t_n, x_k)}{\partial t^3} \Psi_k^n| = \Delta T_{t,l}^{sup}.$$

If we a sufficient number of smooth derivatives ($m = 3$) we have,

$$\delta T = -\frac{C\rho}{2} \sum_{k=1,\, n=2}^{N_x\ N_t} (\tau \frac{\partial^2 T(t_n, x_k)}{\partial t^2} - \tau \alpha_k^n \frac{\partial^3 T(t_n - \eta_k^n \alpha_k^n \tau, x_k)}{\partial t^3} \Psi_k^n h_k \tau, \qquad (16)$$

$$\Delta T_{t,l}^{sup} = \frac{C\rho}{2} \sum_{k=1,\, n=2}^{N_x\ N_t} |\tau^2 \frac{\partial^3 T(t_n - \eta_k^n \alpha_k^n \tau, x_k)}{\partial t^3} \Psi_k^n | h_k \tau. \qquad (17)$$

Estimation of error due to space discretization,

$$\delta T_x = -\frac{\lambda}{12} \sum_{k=1,\, n=2}^{N_x\ N_t} h_k^3 \frac{\partial^4 T(t_n, x_k)}{\partial x^4} \Psi_k^n \tau - \qquad (18)$$

$$\frac{\lambda}{24} \sum_{k=1,\, n=2}^{N_x\ N_t} h_k^3 (\frac{\partial^5 T(t_n, x_k)}{\partial x^5} \beta_k^n - \frac{\partial^5 T(t_n, x_k)}{\partial x^5} \gamma_k^n) \Psi_k^n h_k \tau,$$

$$\Delta T_x^{corr} = -\frac{\lambda}{12} \sum_{k=1,\, n=2}^{N_x\ N_t} h_k^3 \frac{\partial^4 T(t_n, x_k)}{\partial x^4} \Psi_k^n \tau, \tag{19}$$

$$\frac{\lambda}{24} \sum_{k=1,\, n=2}^{N_x\ N_t} h_k^3 (\frac{\partial^5 T(t_n, x_k)}{\partial x^5} \beta_k^n - \frac{\partial^5 T(t_n, x_k)}{\partial x^5} \gamma_k^n) \Psi_k^n h_k \tau < \Delta T_{x,1}^{sup} =$$

$$\sum_{k=1,\, n=2}^{N_x\ N_t} h_k^4 | \frac{\partial^5 T(t_n, x_k)}{\partial x^5} \Psi_k^n | \tau.$$

Using analytical solution of temperature equation,

$$T_{an}(x,t) = \frac{Q}{2\sqrt{\frac{\pi\lambda}{C\rho}(t-t_0)}} \exp\left(\frac{-(x-\xi)^2}{4\lambda/(C\rho)(t-t_0)}\right). \tag{20}$$

Figs 4- 6 illustrate the comparison between

- analytic
- finite difference
- corrected finite-difference solution

and error bounds for $h = 10^{-4}$m, $\Delta t = 1.0$ seconds in different zones.

Figure Captions

Fig. 1. Initial and final temperature distribution. 1 - Initial temperature, 2- Final temperature.

Fig. 2. Temperature isolines

Fig. 3. Adjoint temperature isolines

Fig. 4. The comparison of numerical and analytical solutions in zone A (Fig. 1). 1- analytical, 2-numerical, 3-refined solution, 4- upper bound, 5- lower bound

Fig. 5. The comparison of numerical and analytical solutions in zone B. 1- analytical, 2-numerical, 3- refined solution, 4- upper bound, 5 lower bound

Fig. 6 The comparison of numerical and analytical solutions in zone C. 1- analytical, 2-numerical, 3- refined solution, upper bound, 5- lower bound

Fig. 7. Initial and final temperature distribution. 1- Initial temperature, 2- Final temperature

Fig. 8. The refined solution and error bounds in comparison with finite-difference and analytical solution. Zone A (Fig. 7). 1- analytical, 2-numerical 3- refined solution, 4- lower bound, 5 upper bound

Fig. 9. The refined solution and error bounds in comparison with finite-difference and analytical solution. Zone B (Fig. 7). 1- analytical, 2-numerical, 3- refined solution, 4-lower bound, 5- upper bound

Fig. 10. Initial and final temperature distribution. 1- Initial temperature, 2- Final temperature, A-zone of estimation

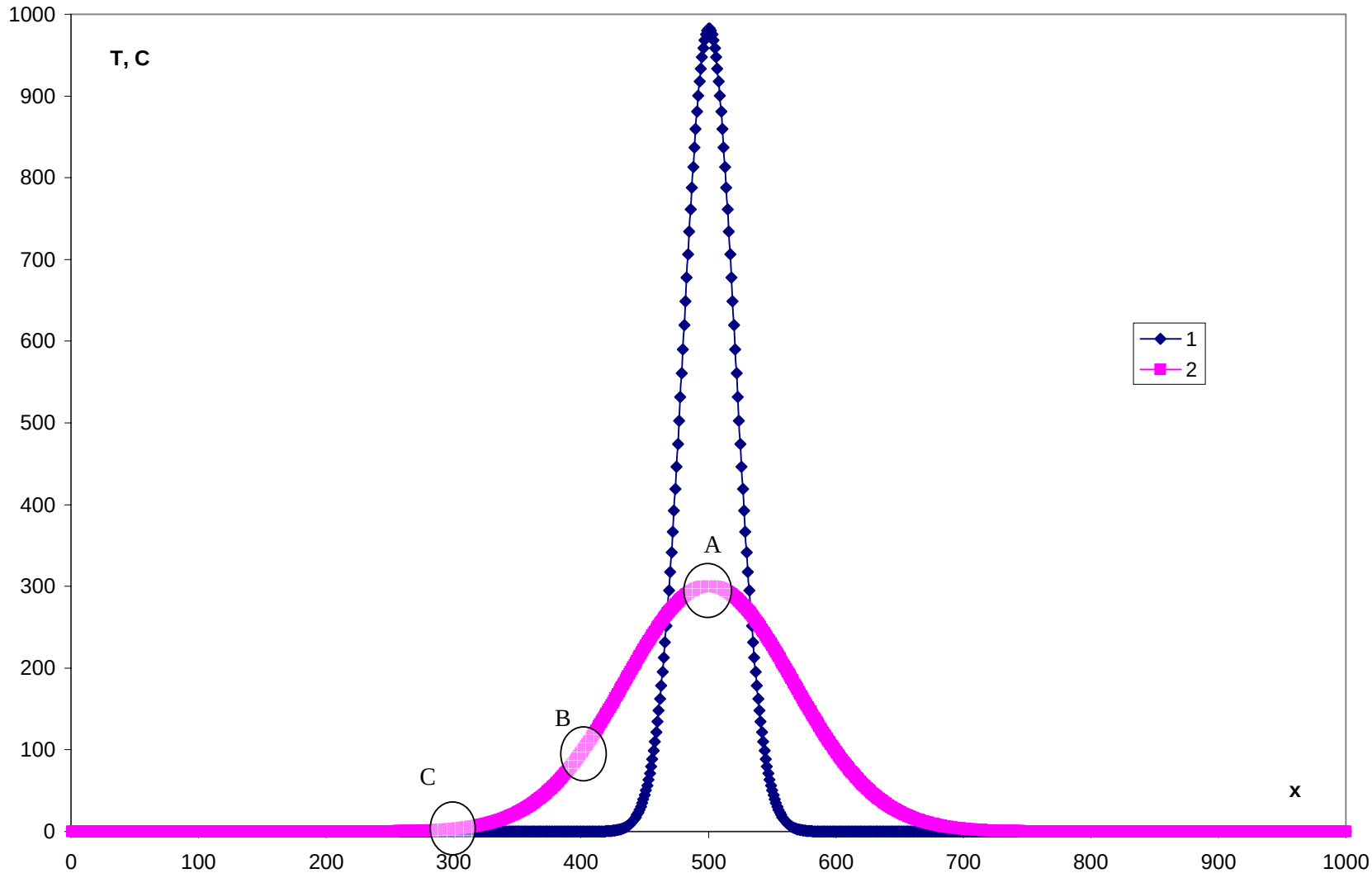
T, C
1000
900
800
700
600
500
400
300
200
100
0
0
100
200
300
400
500
600
700
800
900
1000
x
1
2
A
B
C

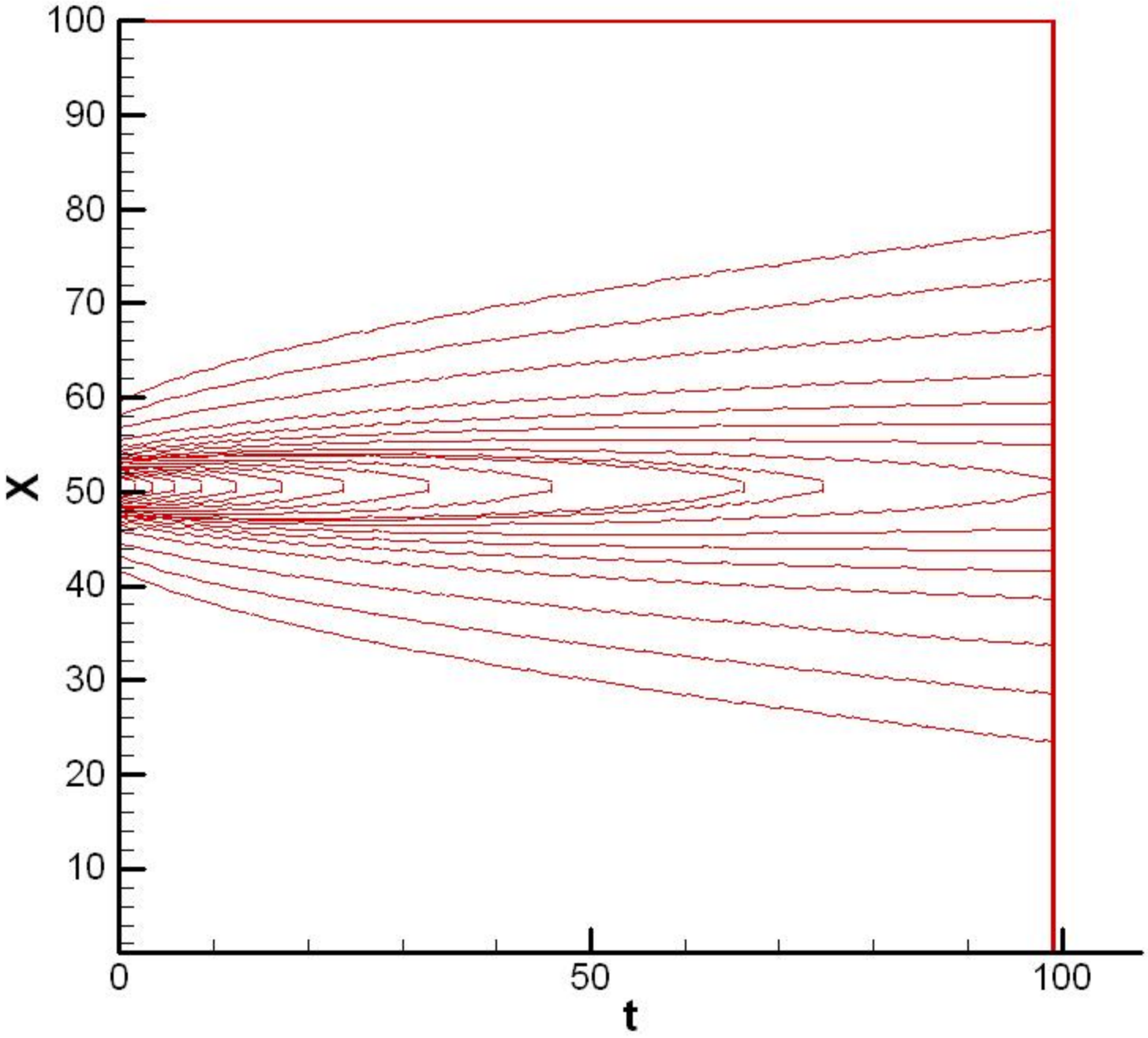
100
90
80
70
60
50
40
30
20
10
X
0
50
100
t

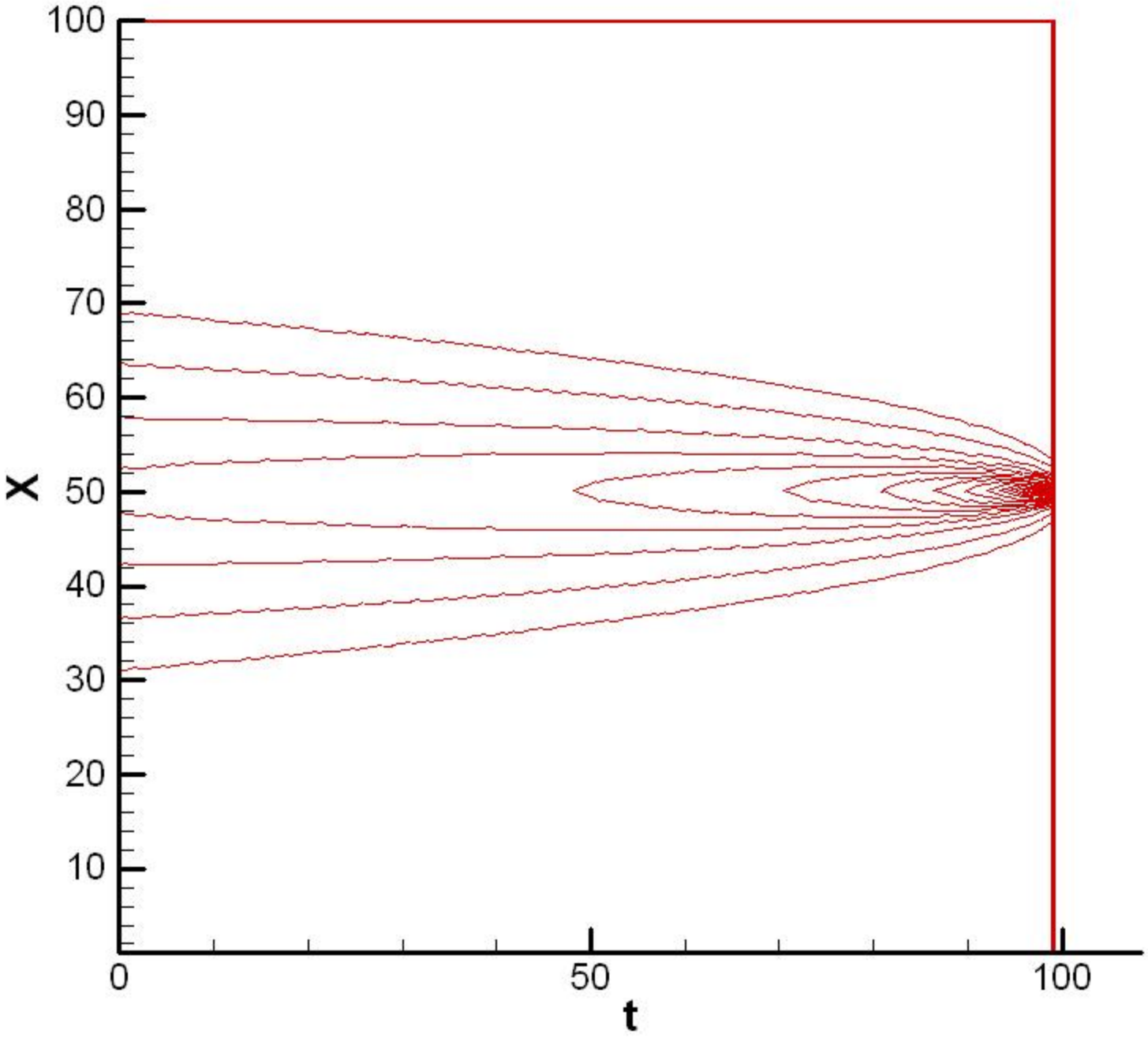
100
90
80
70
60
50
40
30
20
10
X
0
50
100
t

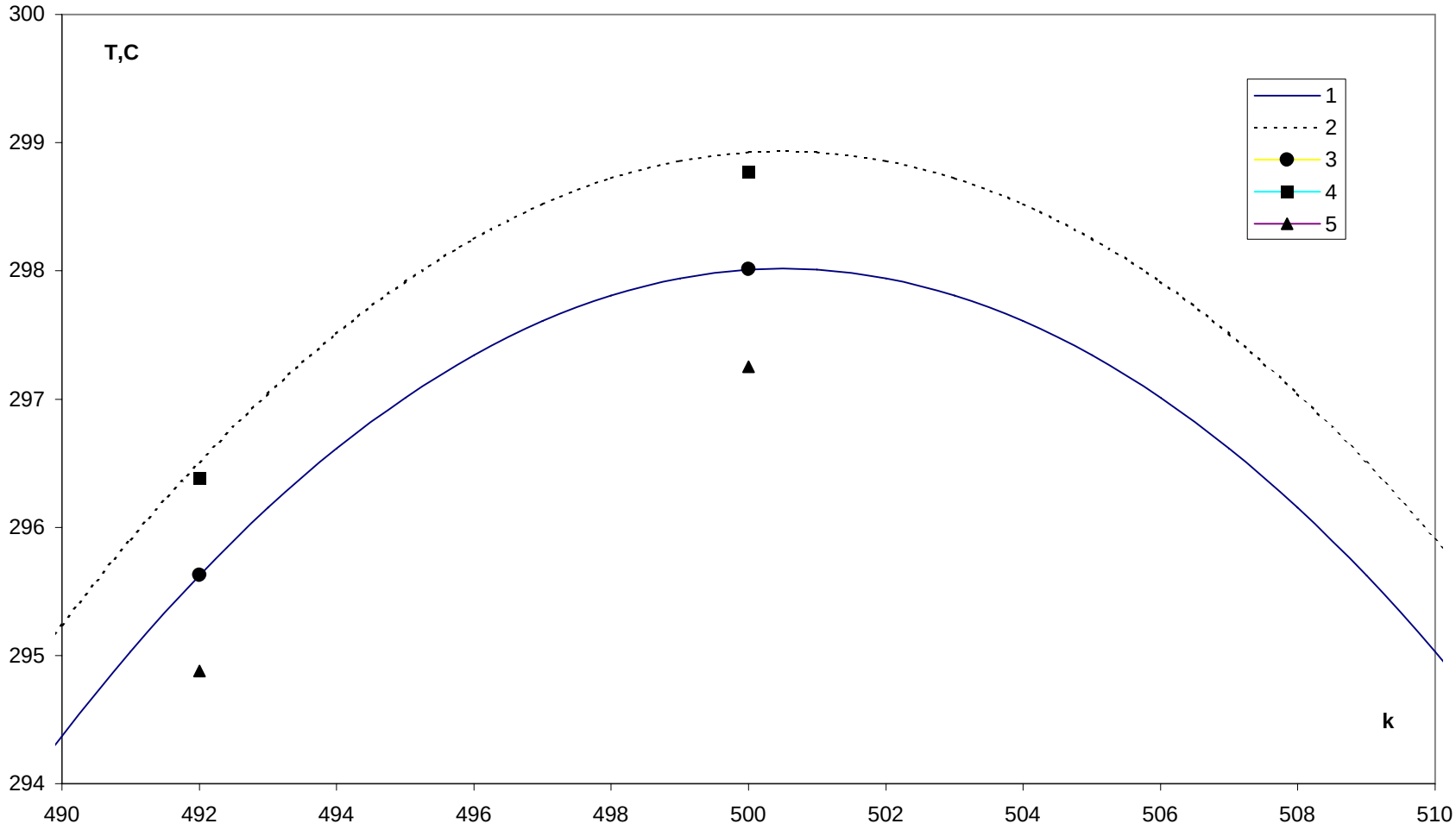
T,C
300
299
298
297
296
295
294
490
492
494
496
498
500
502
504
506
508
510
k
1
2
3
4
5

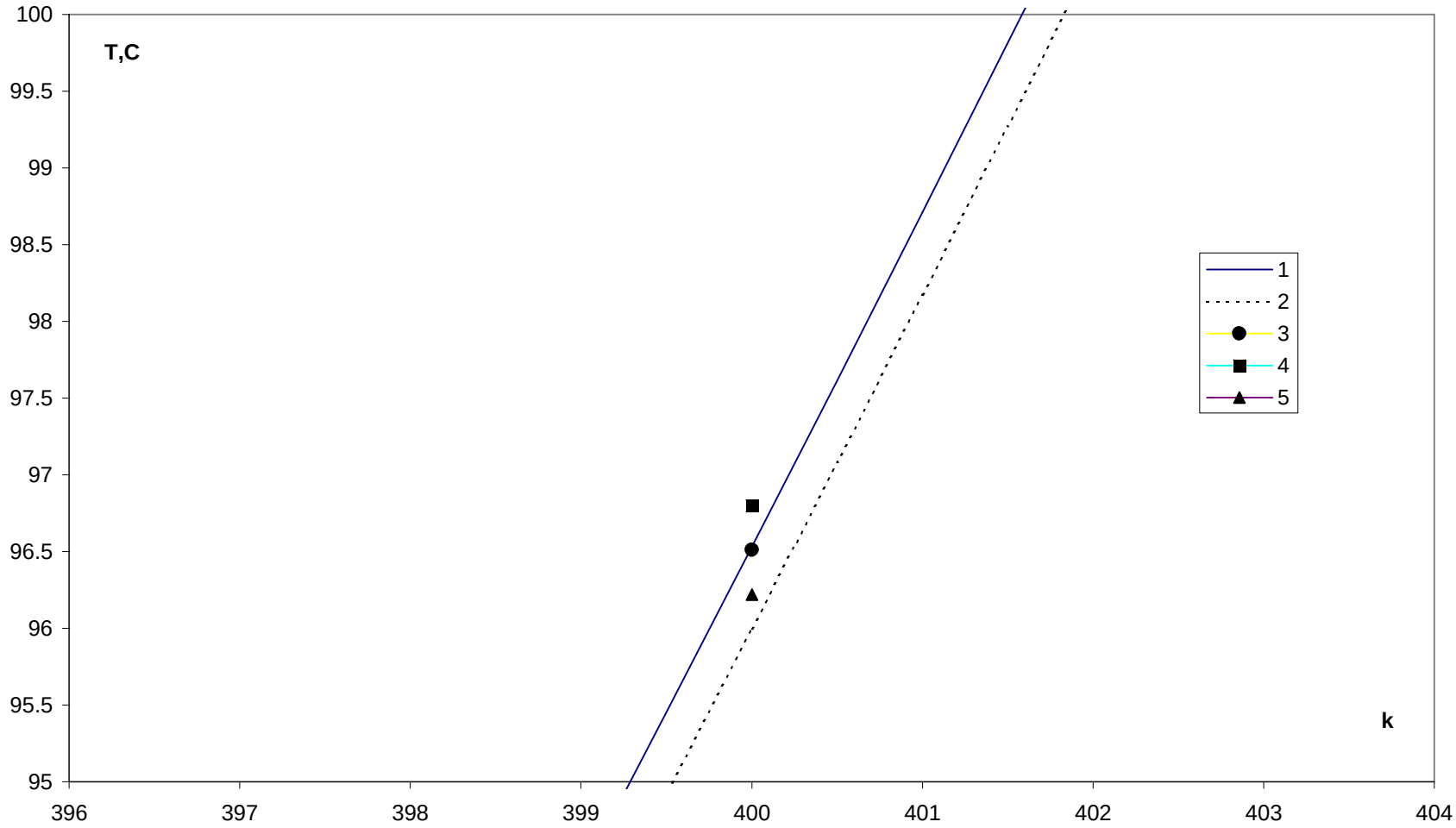
T,C
100
99.5
99
98.5
98
97.5
97
96.5
96
95.5
95
396
397
398
399
400
401
402
403
404
k
1
2
3
4
5

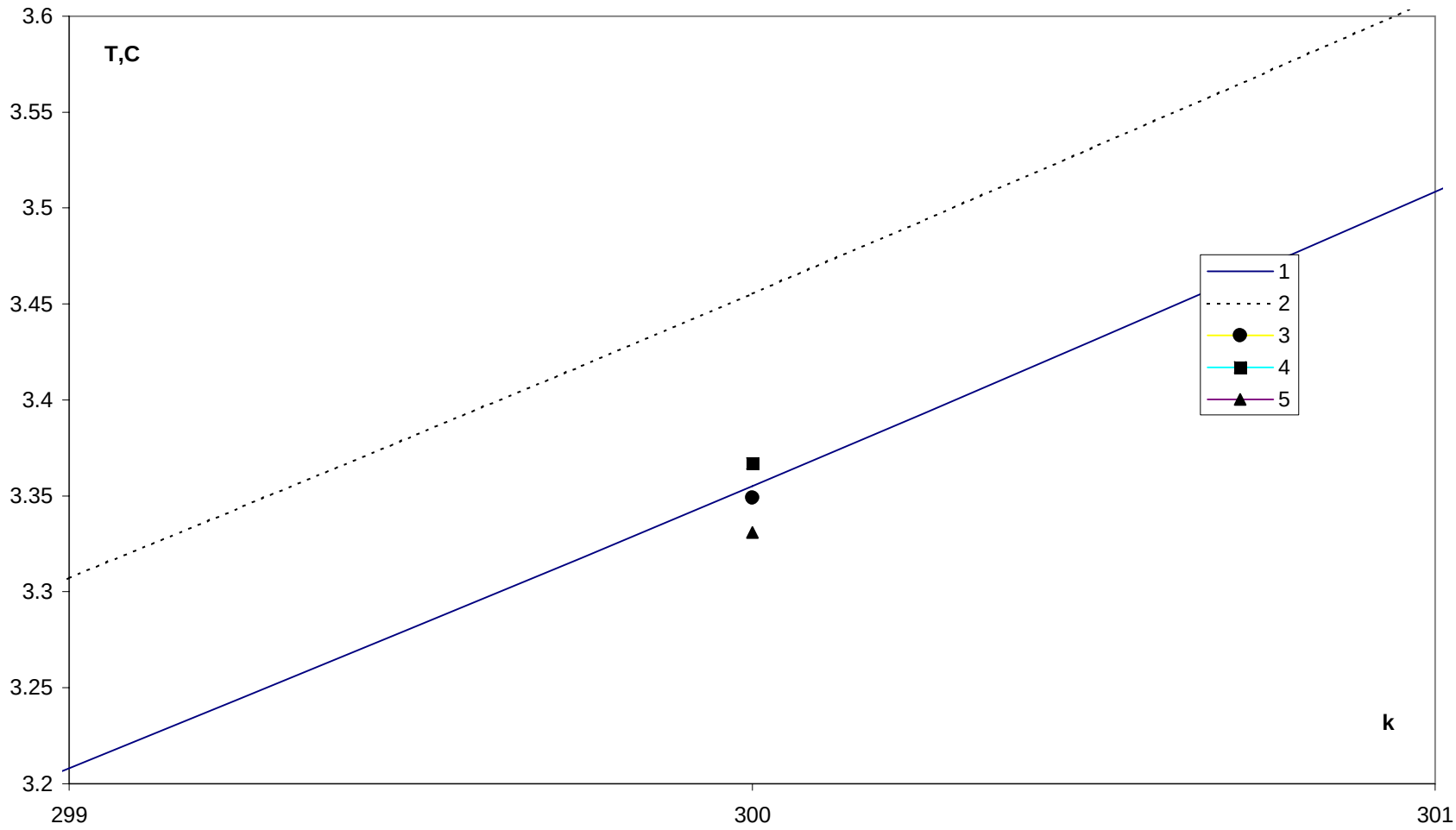
T,C
3.6
3.55
3.5
3.45
3.4
3.35
3.3
3.25
3.2
299
300
301
k
1
2
3
4
5

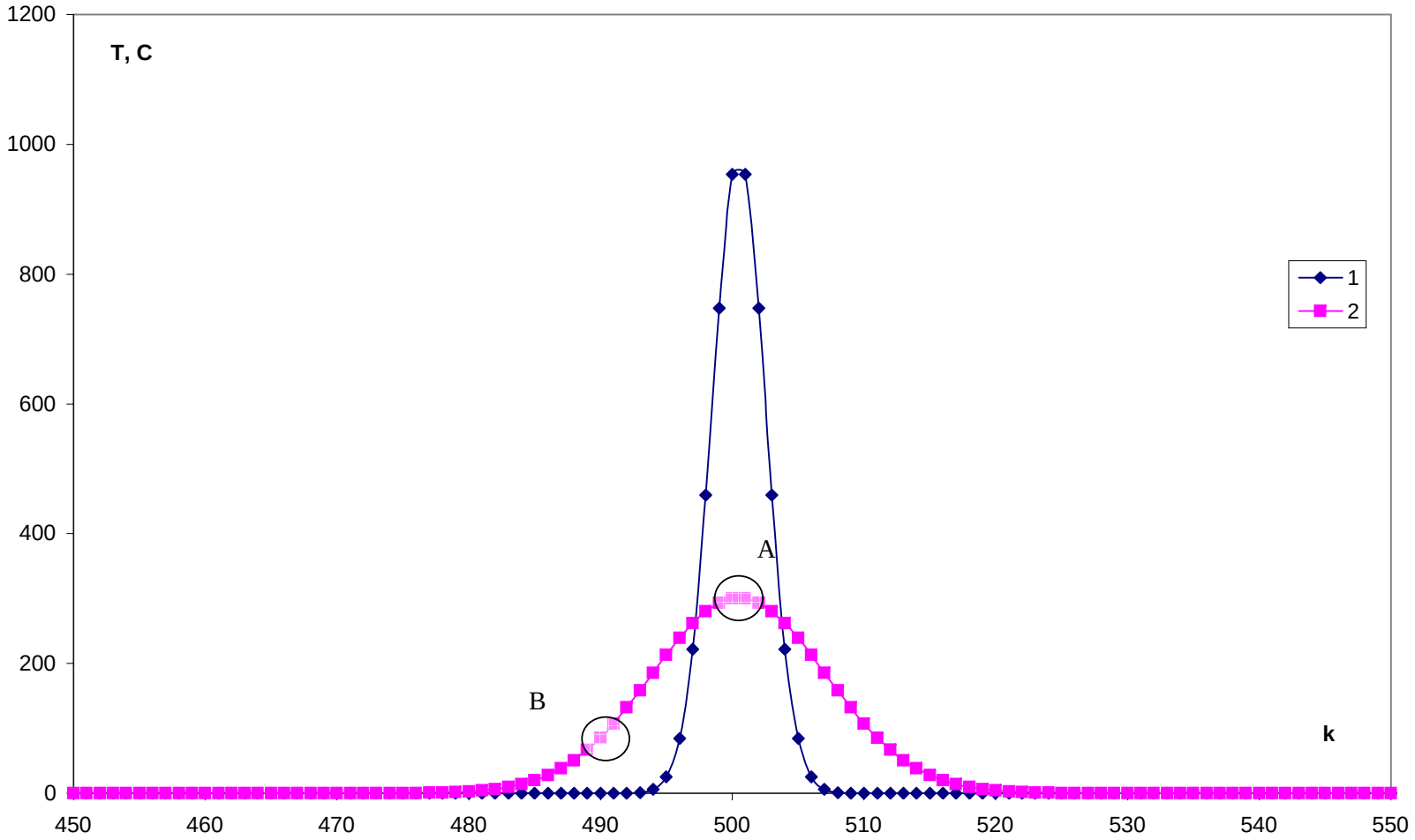
T, C
1200
1000
800
600
400
200
0
450
460
470
480
490
500
510
520
530
540
550
1
2
A
B
k

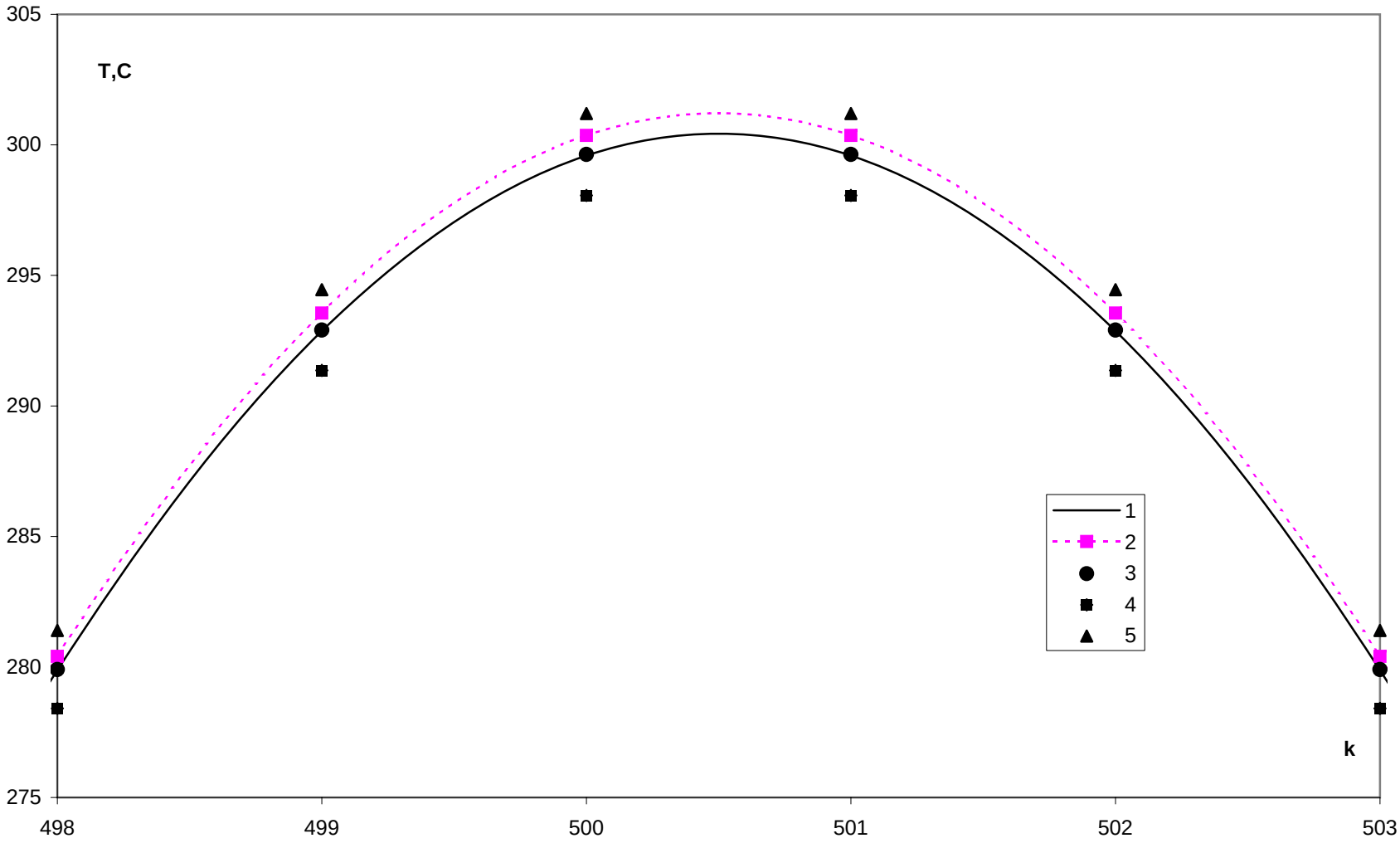
T,C
305
300
295
290
285
280
275
498
499
500
501
502
503
k
1
2
3
4
5

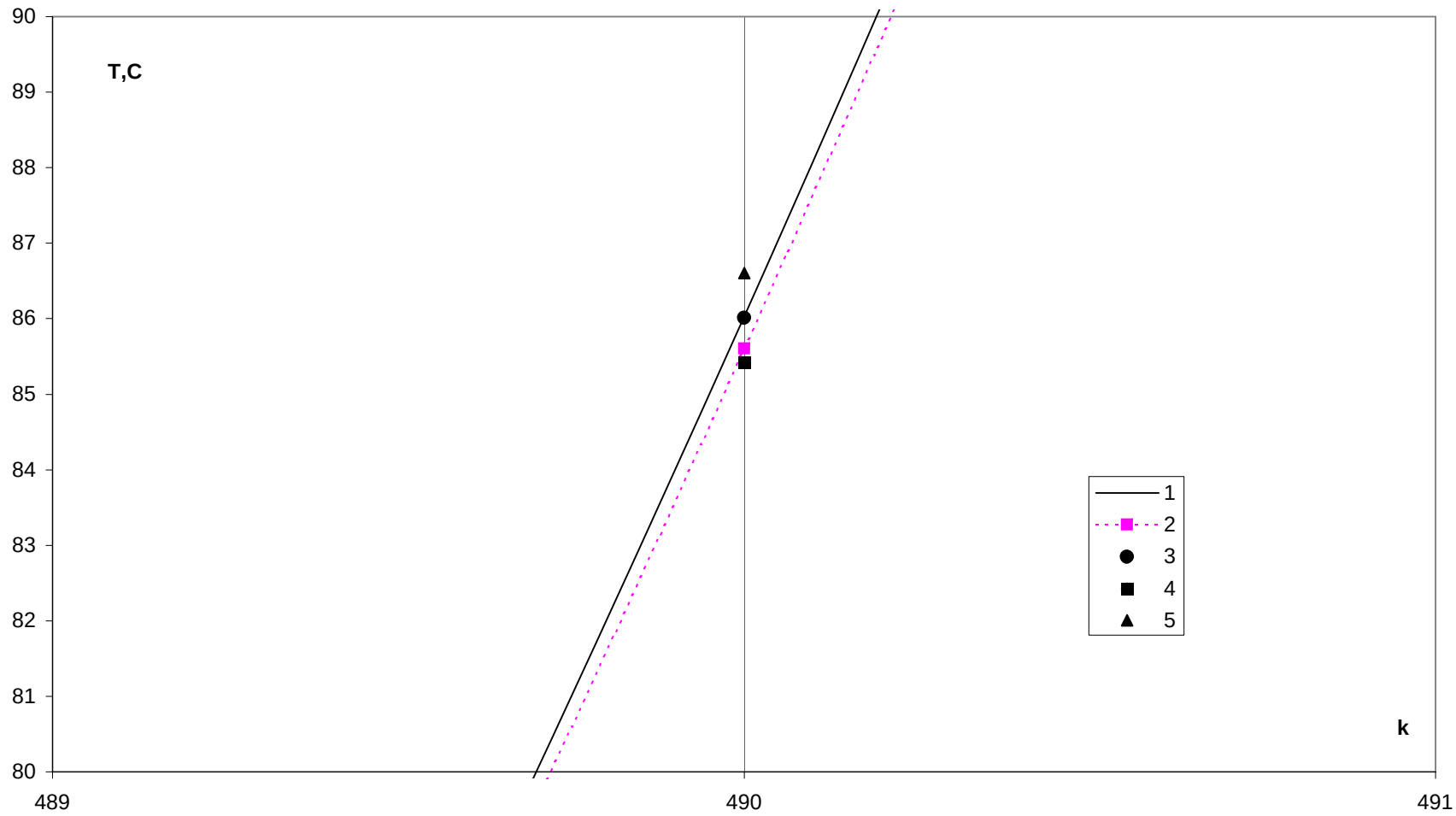
T,C
90
89
88
87
86
85
84
83
82
81
80
489
490
491
k
1
2
3
4
5

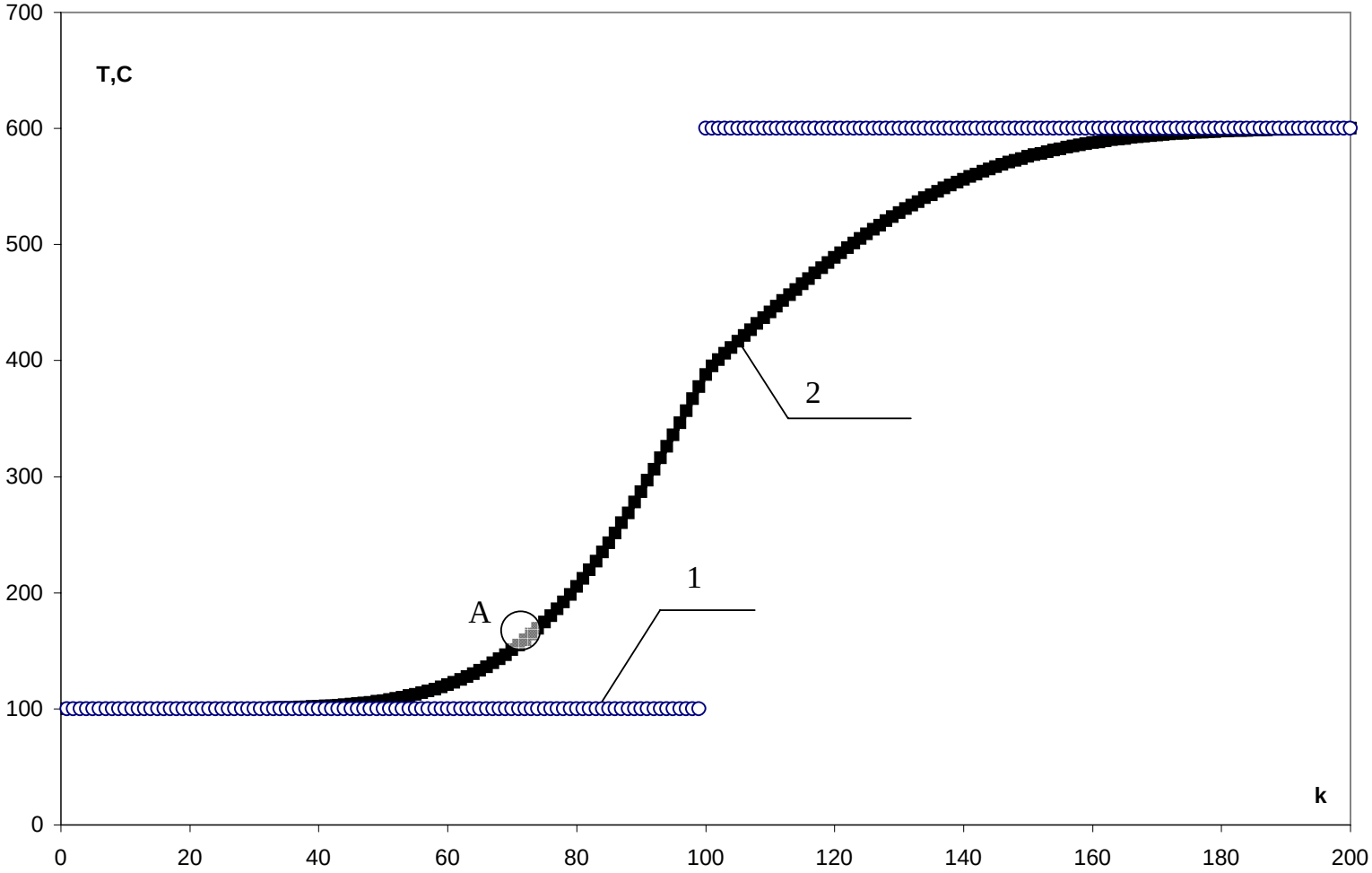
T,C
700
600
500
400
300
200
100
0
0
20
40
60
80
100
120
140
160
180
200
k
A
1
2

Conclusions for this Section

Numerical tests demonstrate that pointwise error of f.d. solution of heat conduction equation may be reduced using differential approximation of finite-difference scheme in conjunction with the adjoint equations.

- This approach may be used for other output temperature functionals with preset levels of accuracy,
- CPU time required for refined and for the error bound calculation is equal to CPU time required for temperature calculation on a mesh of same resolution and same size.

Use of Adjoint correction for adaptive mesh refinement in 3-D time dependent models

Examples will be presented related to dynamically adaptive meshes for Imperial College Ocean Model.

- Use of sensitivity functional taken with respect to solution variables, used as basis from which error measures are derived.
- Error measures act to predict those areas of model domain where solution should be changed- and involve solution of both forward and adjoint problems.
- Mesh quality is assessed with respect to a Riemann metric tensor embodying the error measure.
- The result is a mesh in which each finite element node has approximately(subject to boundary conforming constraints) equal error contribution to the output functional.

- Aim: to exploit use of unstructured dynamically adapting meshes in both horizontal and vertical directions.
- Use geometrical flexibility of f.e.m. mesh to conform well to both topography and ocean coast lines.
- Use various 'a-posteriori error-measures in which same set of equations are solved for the errors with sources provided by residuals of the governing equations.
- Aim of goal based error measure is to construct (and design error measure) of a quantity deemed important in the problem- and to design the error measure to optimize accuracy of the particular functional output. The resulting constructed mesh is to achieve this level of accuracy with minimal computational resources.

- In oceanographic sense the goal functional can be either an observation from a buoy , some measure of the dynamics of the system i.e. some integral of vorticity or strength of the thermohaline circulation, etc.
- Since adjoint solution is typically calculated for data assimilation purposes - this approach provides an additional use for the adjoint model information, i.e. to adapt f.e.m. mesh and provide indicators of the accuracy of output functional or goal.
- These methods provide also framework for optimizing accuracy of inverse problem.
- One can use readily accessible (in simulation codes)discretized equations
- use of metric tensor obtained vis sensitivity analysis to adapt 3-D meshes of unstructured tetrahedral elements.

- Once an appropriate output functional-representative of significant dynamics of the flow was found -the method removes the need to allocate varying priorities on resolving various fields(velocity,pressure and density)at various locations and times.
- Advantages include
- Superconvergence of goal with mesh adaptivity
- Ability to assign bounds on accuracy of the goal
- Possibility of improving accuracy of the goal

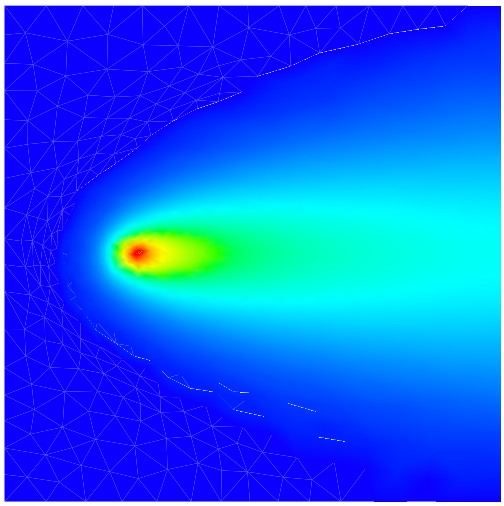

Fig. 8. Solution to the forward problem.

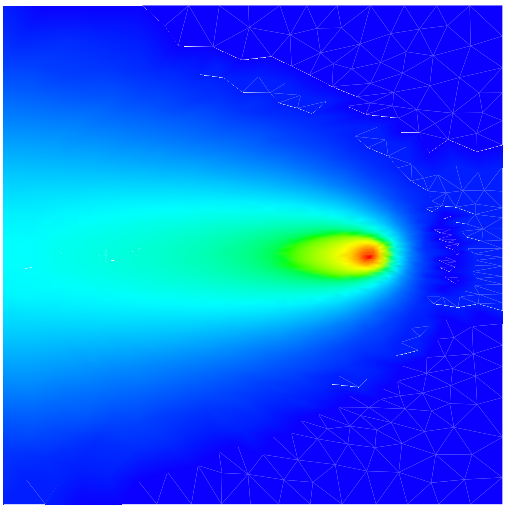

Fig. 9. Solution of the adjoint problem.

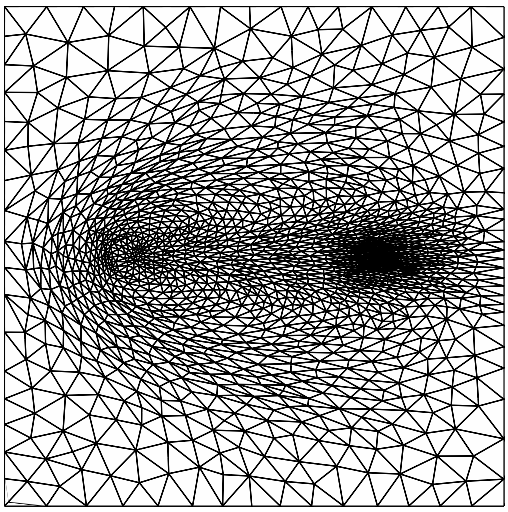

Fig. 10. Mesh resulting from the use of the forward metric tensor to adapt the initial mesh. 3296 nodes, 10467 elements.

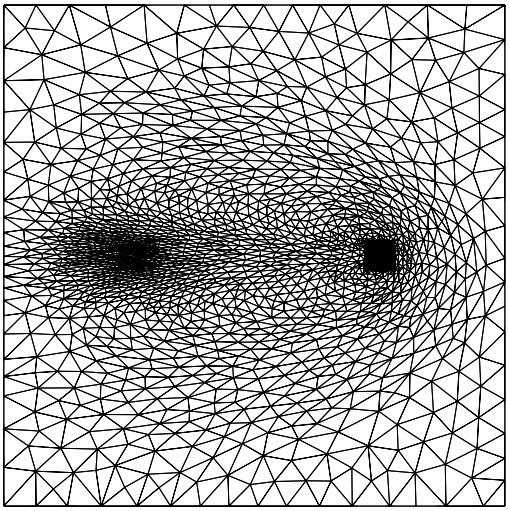

Fig. 11. Mesh resulting from the use of the adjoint metric tensor to adapt the initial mesh. 8061 nodes, 27217 elements.

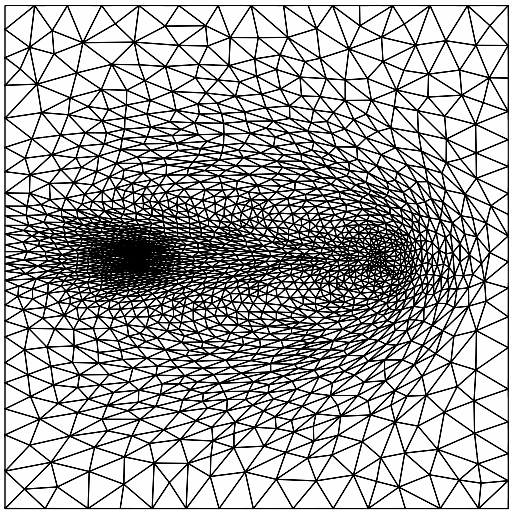

Fig. 14. Mesh resulting from the use of the modified adjoint metric tensor to adapt the initial mesh. 3216 nodes, 10150 elements.

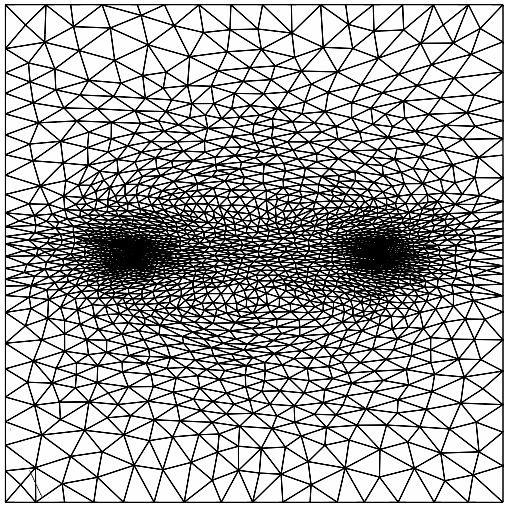

Fig. 15. Mesh resulting from the use of a superposition of forward and modified adjoint metric tensors to adapt the initial mesh. 3576 nodes, 11023 elements.

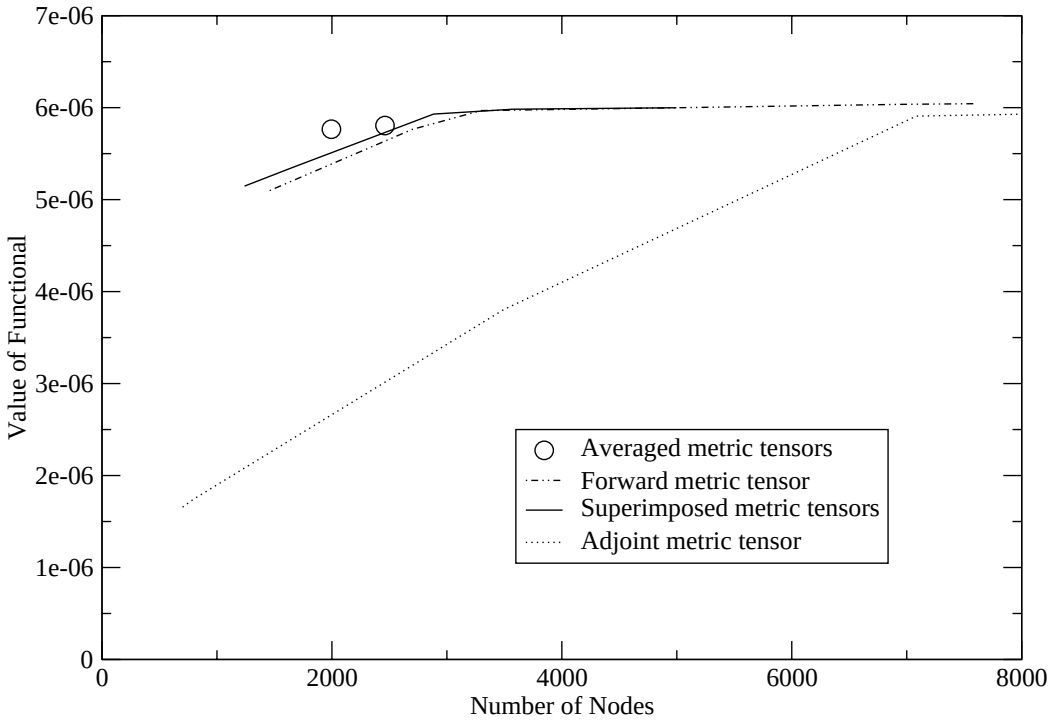

Fig. 18. Graph comparing the value of the functional for mesh adapted using different metric tensors.

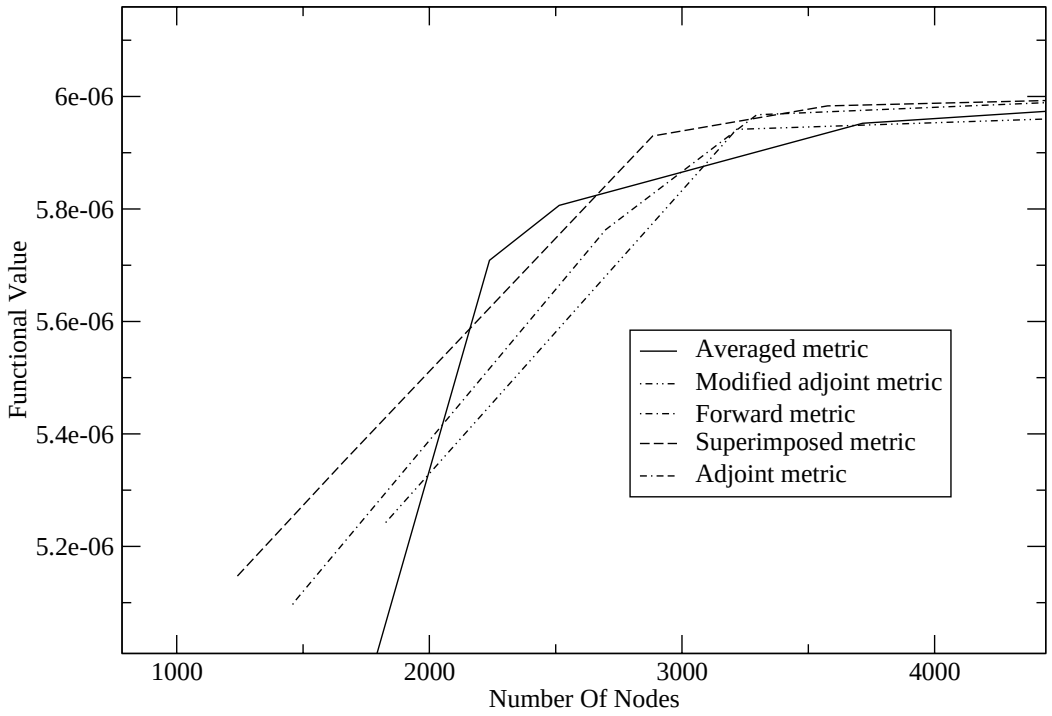

Fig. 19. Graph comparing the value of the functional for mesh adapted using different metric tensors, blowup around area of 2000–4000 nodes.

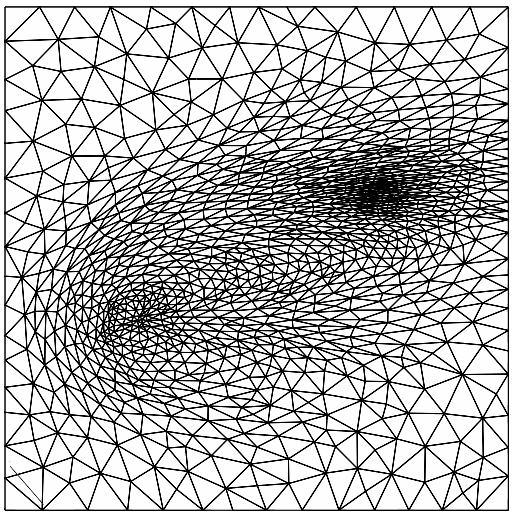

Fig. 20. Mesh adapted using forward metric tensor for an offset source and detector. 2578 nodes, 8453 elements.

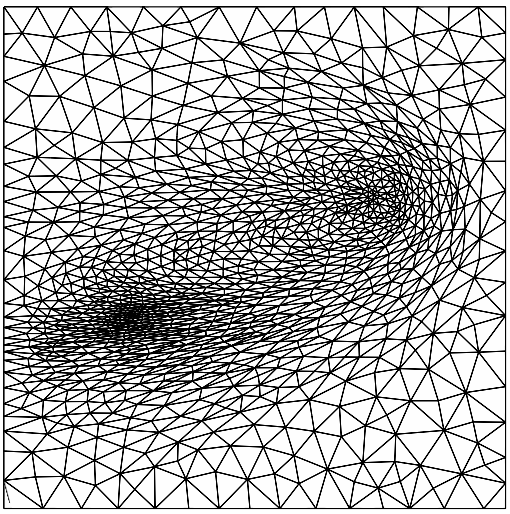

Fig. 21. Mesh adapted using modified adjoint metric tensor for an offset source and detector. 2643 nodes, 8655 elements.

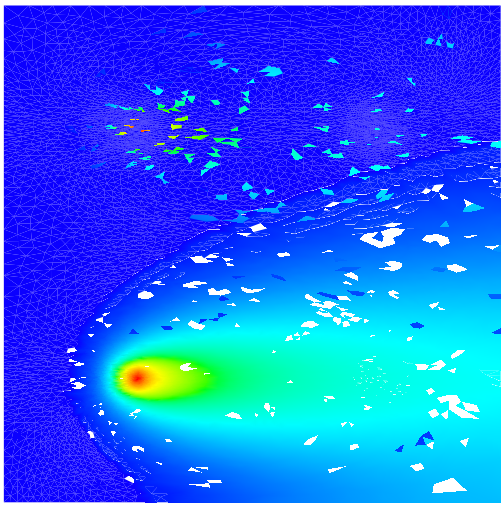

Fig. 24. Solution for first of two temperature fields.

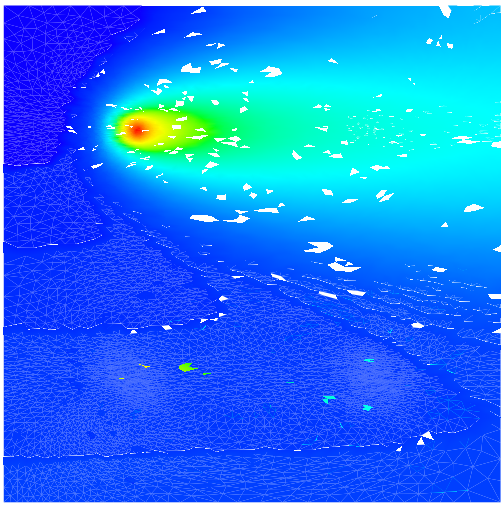

Fig. 25. Solution for second of two temperature fields.

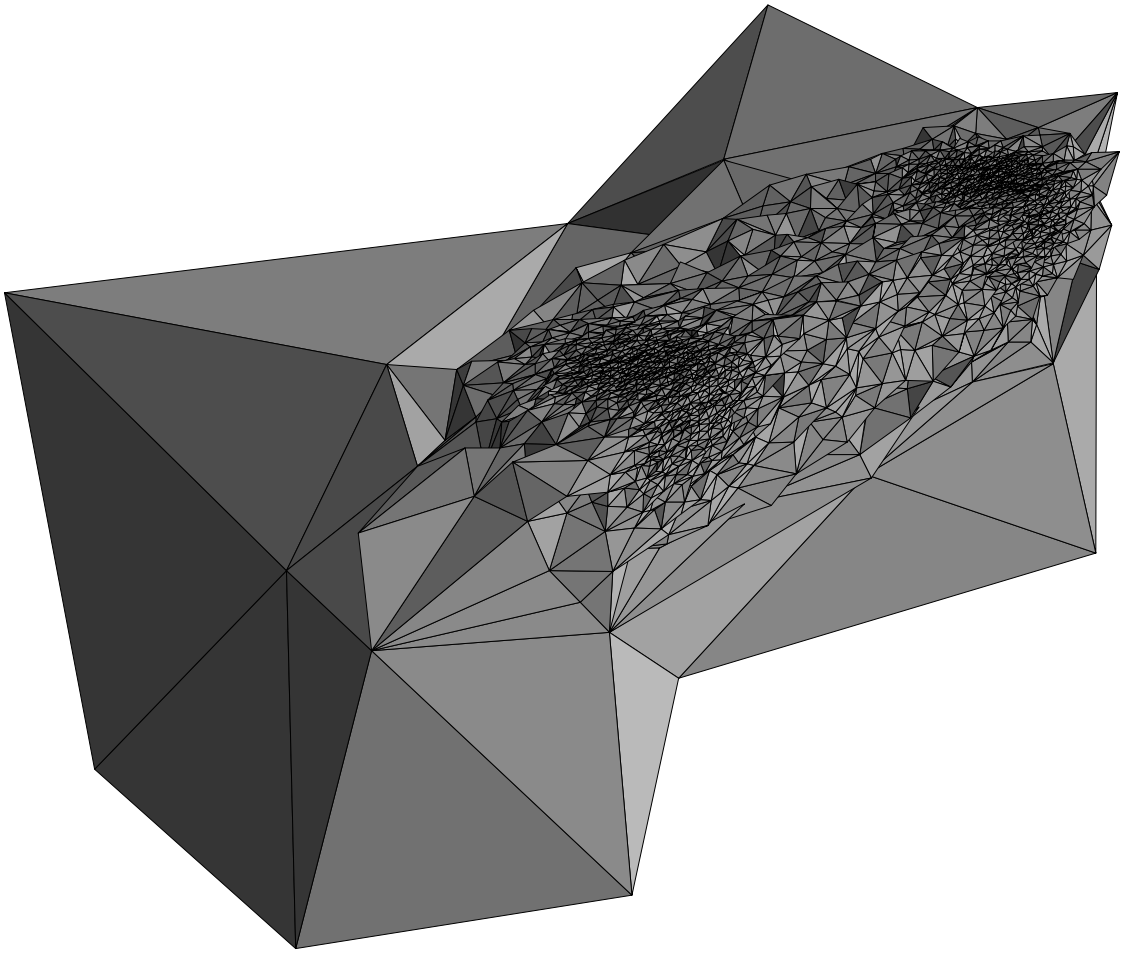

Fig. 26. Adaptation in three-dimensions, elements where $x > 2$ and $z > 2$ are removed. 28974 nodes, 165049 elements.

$$\nabla \cdot \mathbf{u} = 0. \tag{6.2}$$

Where $\mathbf{u} = (u, v, w)$ represents the 3D velocity and p is the perturbation pressure. Here u, v and w are the velocity components in the x-, y- and z-directions respectively. The rotation vector is $\mathbf{\Omega}$ and takes the form $\mathbf{\Omega} = \left(0, 0, \frac{f}{2}\right)^T$, where f is the Coriolis parameter. The viscous terms are represented by the stress tensor $\boldsymbol{\tau}$. More details of the numerical basis of the model can be found in [4].

6.2.2 Choice of functional

A functional can be defined in terms of the vorticity, as the problem is 2D only one component of the vorticity,

$$\zeta = \left(\frac{\partial v}{\partial x} - \frac{\partial u}{\partial y}\right), \tag{6.3}$$

is non-zero. The rationale for basing functionals around vorticity stems from both the physics but also the ability to represent the vorticity numerically. Thus an appropriate functional can be defined as,

$$f\left(u, v\right) = \frac{1}{2}\zeta^2. \tag{6.4}$$

To initialize the adjoint problem (see section 6.1) the source terms $\frac{\partial F}{\partial \Psi}$ must be calculated. When time stepping is used the functional from as defined in chapter 4 can be defined as total enstrophy at time level $n + L$,

$$F = \frac{1}{2}\int \left(\zeta^{(n+L)}\right)^2 dV = \frac{1}{2}\int \left(\left(\frac{\partial v}{\partial x}\right)^{(n+L)} - \left(\frac{\partial u}{\partial y}\right)^{(n+L)}\right)^2 dV, \tag{6.5}$$

in which L is the number of time steps used to form the error measure. The aim of using the functional defined by equation 6.5 is to optimize the accuracy of the functional at the end of time step $\widehat{\Delta\mathcal{T}}$ (time interval between two consecutive mesh adaptations), or taking

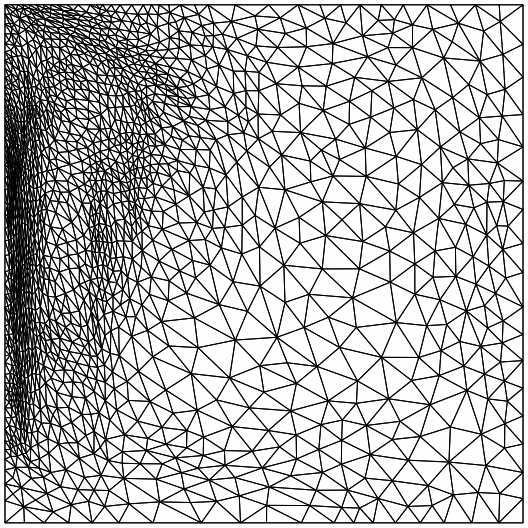

Figure 6.16: Mesh adapted to optimize accuracy of functional F at day 122.5. 2543 nodes.

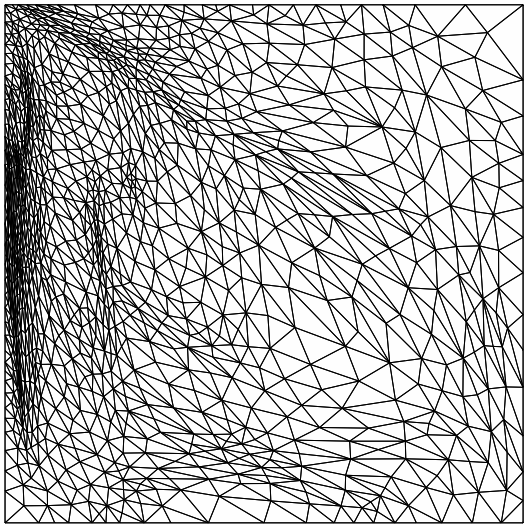

Figure 6.17: Mesh adapted to optimize accuracy of functional F at day 147.5. 2133 nodes.

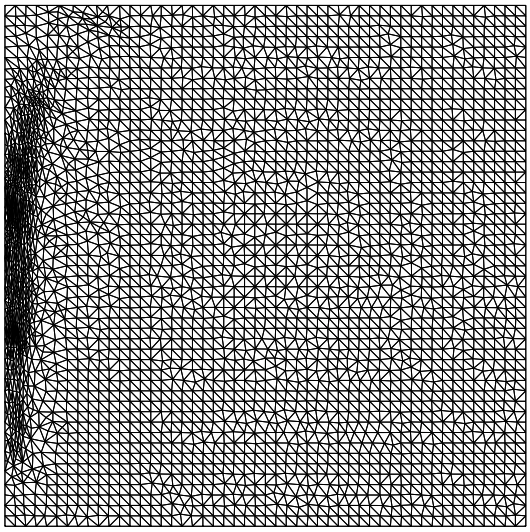

Figure 6.18: Mesh adapted to optimize accuracy of functional F at day 102.5. 6894 nodes, 20185 elements. $Re = 1000$.

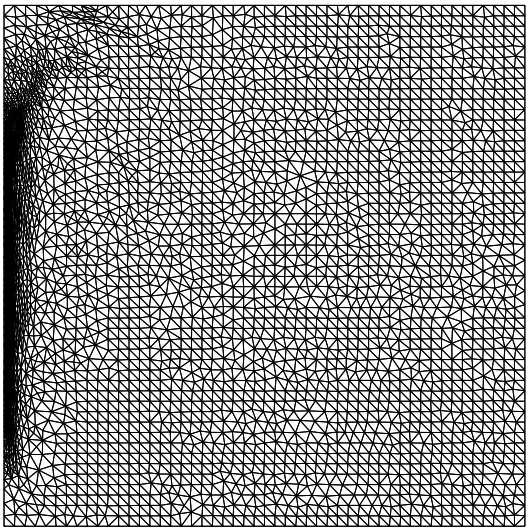

Figure 6.19: Mesh adapted to optimize accuracy of functional F at day 107.5. 7057 nodes, 20445 elements. $Re = 1000$.

7.1.1 Functional representation of flow dynamics

A functional can be defined in terms of the relative vorticity,

$$\zeta = \begin{pmatrix} \zeta_x \\ \zeta_y \\ \zeta_z \end{pmatrix} = \nabla \times \mathbf{u} = \left(\frac{\partial w}{\partial y} - \frac{\partial v}{\partial z}, \;\; \frac{\partial w}{\partial x} - \frac{\partial u}{\partial z}, \;\; \frac{\partial v}{\partial x} - \frac{\partial u}{\partial y} \right)^T, \tag{7.5}$$

and potential vorticity, $\zeta \cdot \nabla\rho$ as well as gradients of density $\nabla\rho$ and tracer concentration ∇C. The rationale for basing functionals around vorticity and gradients of key quantities stems from their ability to represent the vorticity and gradients numerically. Thus an appropriate functional can be defined as,

$$\begin{aligned} f\left(u, v, w, \rho, C\right) = \\ \frac{1}{2}\mathcal{G}(t)\left(\zeta^T W_\zeta \zeta + (\zeta^T W_{\zeta\rho}\nabla\rho)^2 + (\nabla\rho)^T W_\rho \nabla\rho + (\nabla C)^T W_C \nabla C\right) \\ = \frac{1}{2}\mathcal{G}(t) X \end{aligned} \tag{7.6}$$

in which $\mathcal{G}(t)$ acknowledges the time dependence of the problem and hence the functional. For example, to maximise the accuracy of F at a particular time level $\tau + \widehat{\Delta\mathcal{T}}$ then one could choose

$$\mathcal{G}(t) = \delta\left(\tau + \widehat{\Delta\mathcal{T}} - t\right), \tag{7.7}$$

or to maximise the accuracy of the functional F over a particular time interval $[t_1, t_2]$ then one could choose

$$\mathcal{G}(t) = \frac{H(t|t_1; t_2)}{t_2 - t_1} \tag{7.8}$$

with $H(t|t_1; t_2)$ equal to unity when $t \in [t_1, t_2]$ and zero otherwise.

In equation 7.6 W_ζ, $W_{\zeta\rho}$, W_ρ, and W_C are positive semi-definite weighting matrices. These matrices or tensors may be used to place emphasis on resolving vertical or horizontal structure for example, and are closely analogous to diffusion tensors. However, in

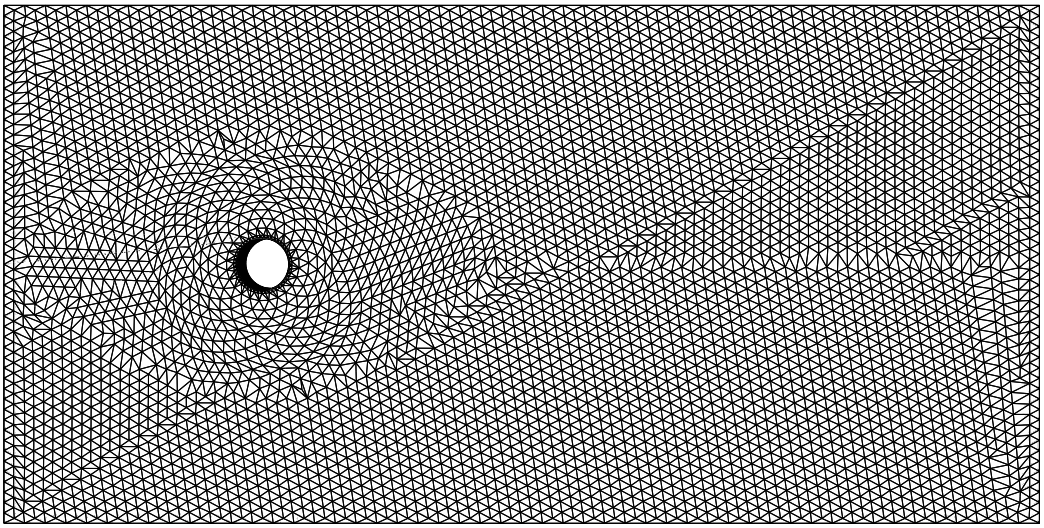

Figure 7.1: Initial mesh for heated cylinder problem.

The functional applied is that defined in equation 7.6, where the required parameters are set as,

$$w_\zeta = 1, \quad w_{\zeta\rho} = 0, \quad w_\rho = 0.$$

The forward metric tensor (equation 4.40) is used in this simulation. The large forward and adjoint time steps for constructing the 34^{th} adaptation of the mesh are considered; at the point of wishing to adapt the mesh a large time step ($\widehat{\Delta\mathcal{T}} = 0.5$) forward is taken, starting from the current velocity and temperature solutions, shown by figures 7.2 and 7.3. The results at the end of the large time step are shown in figures 7.4 to 7.8. The advancement of the solution forward in time through the large time step can be observed in the figures.

The adjoint problem is initialized from the solution to the forward problem by calculating sources which are the differentials of the functional F with respect to the solution parameters. These are detailed for the functional employed in section 7.1.2. As $w_\rho = 0$ and $w_{\zeta\rho} = 0$ in this case, then the differential of the functional is zero. Thus when the adjoint

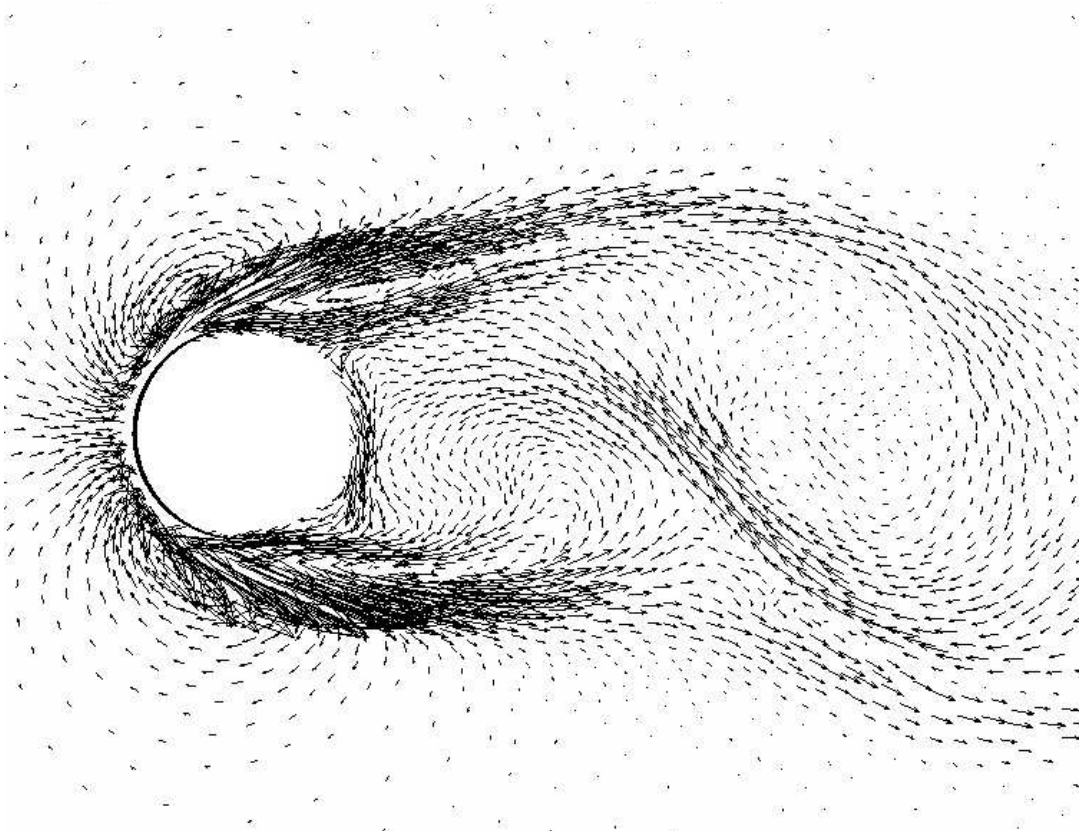

Figure 7.12: Blowup around cylinder of adjoint solution vectors after adjoint timestep relating to 34^{th} adaptation of mesh.

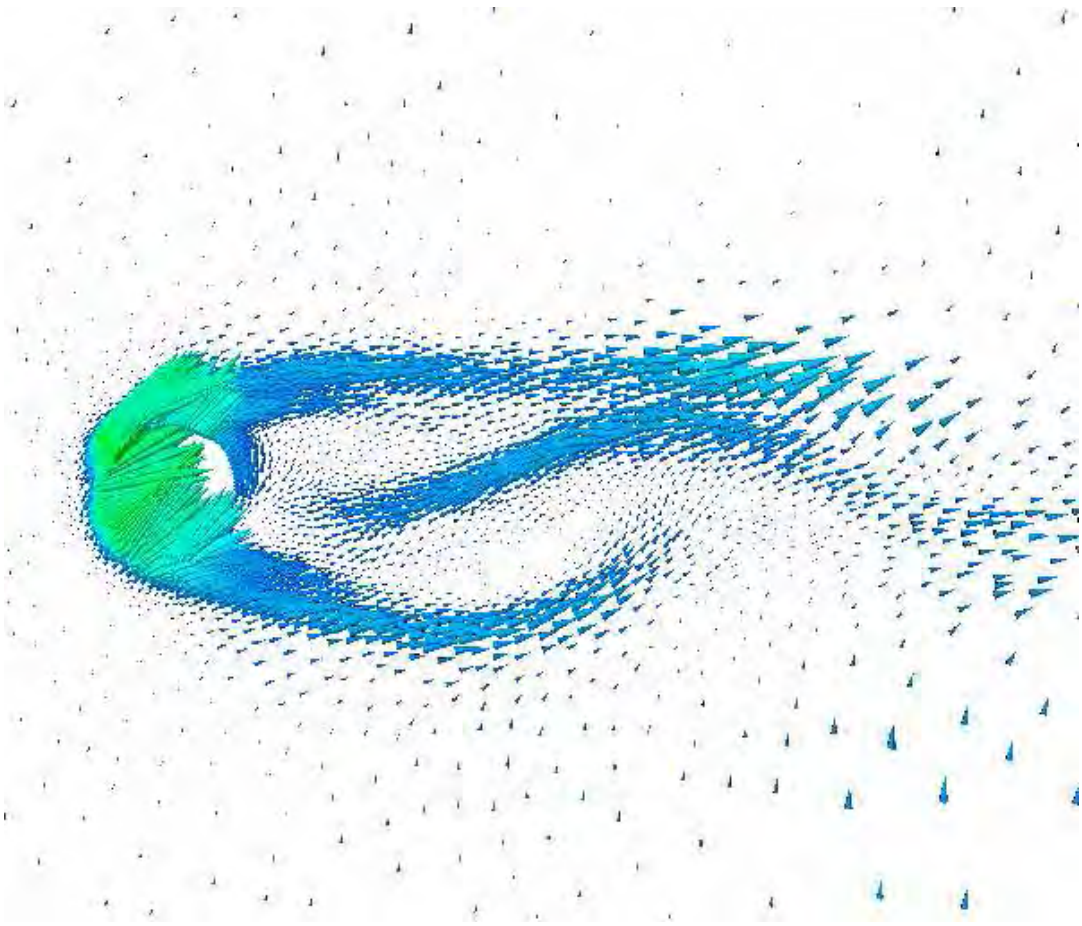

Figure 7.15: Vector representation of adjoint residuals relating to u^* and v^* for 34^{th} adaptation of mesh.

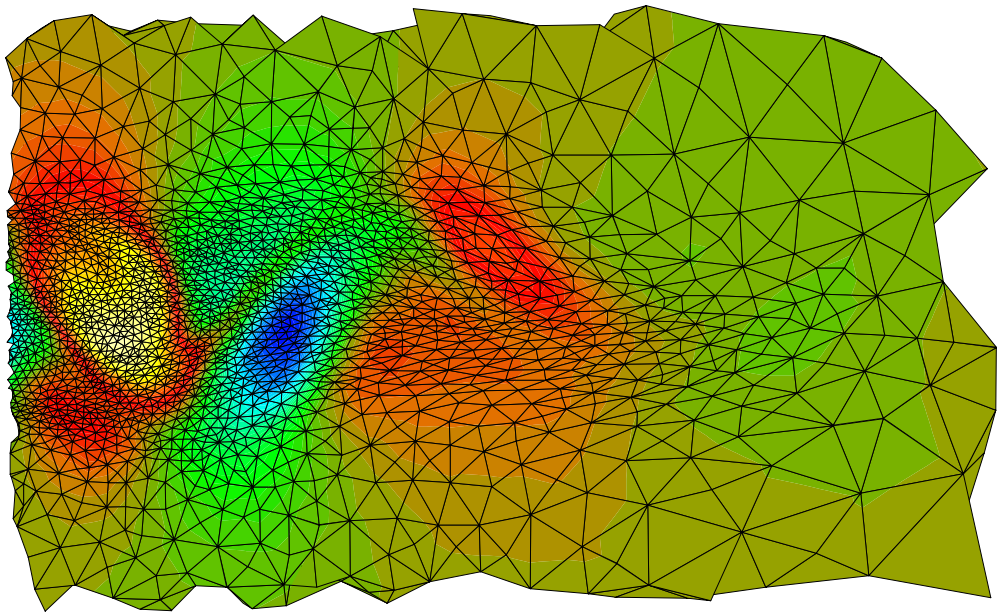

Figure 7.18: Vertical component of vorticity field and 34^{th} adapted mesh.

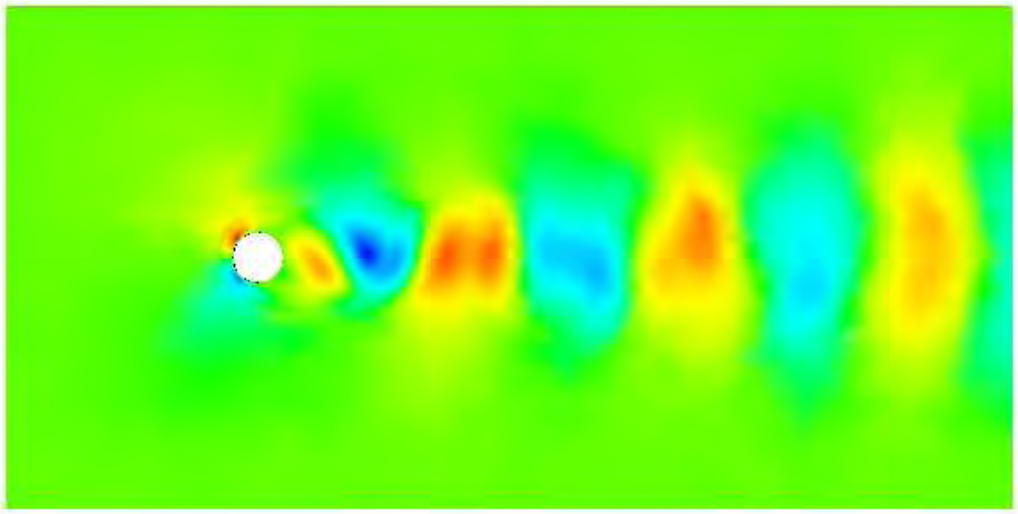

Figure 7.23: u velocity at 100^{th} adapt.

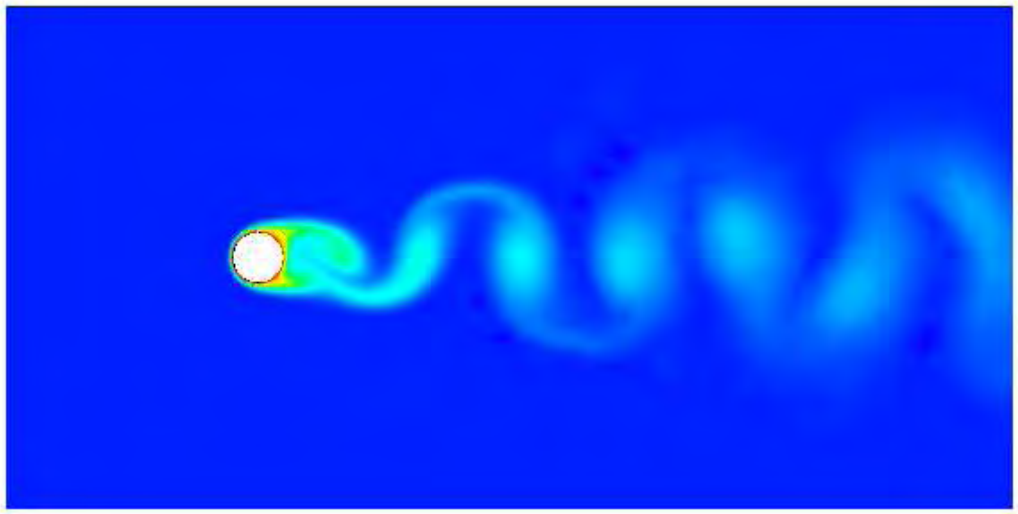

Figure 7.24: Temperature T at 100^{th} adapt.

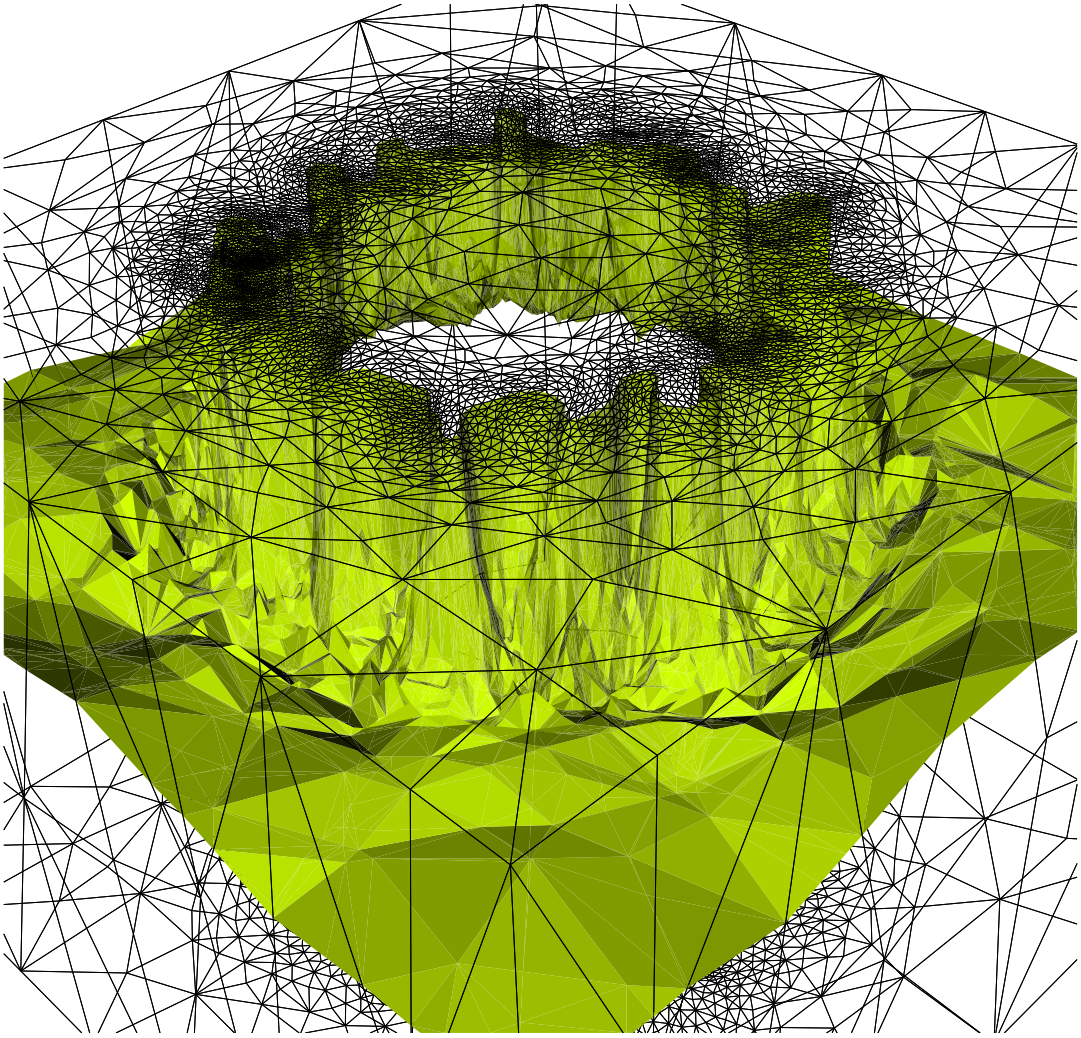

Figure 7.30: Velocity vectors and temperature iso-surface, day 6.

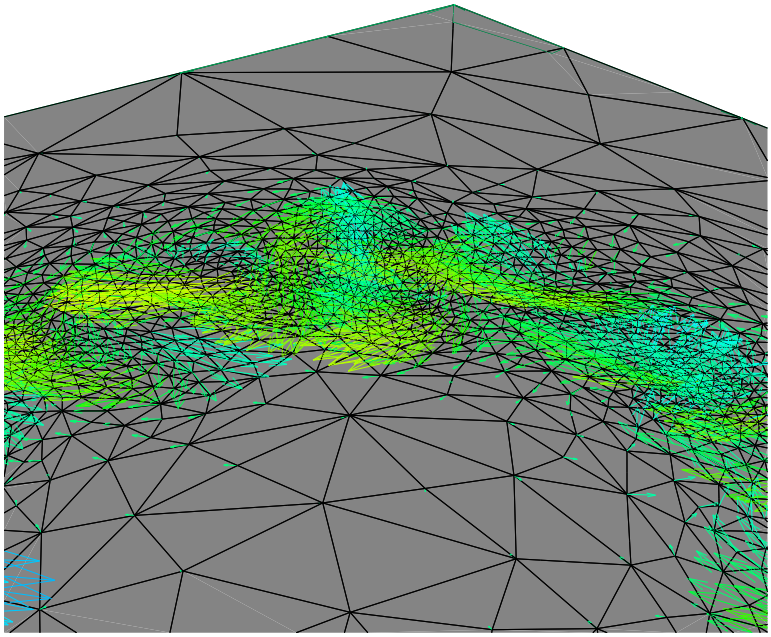

Figure 7.31: Velocity vectors on top surface, day 6.

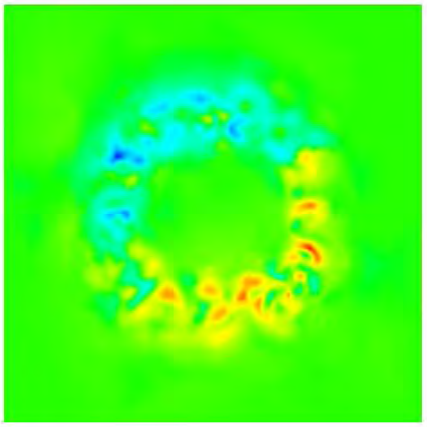

Figure 7.32: Adjoint solution u^*, day 6.

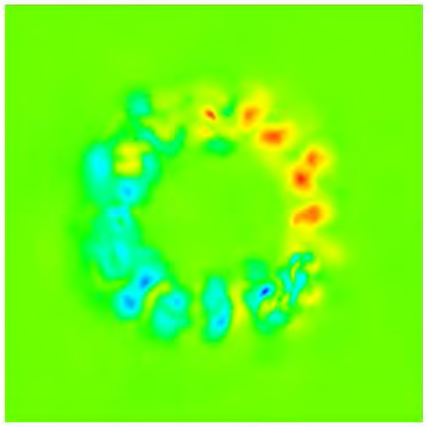

Figure 7.33: Adjoint solution v^*, day 6.

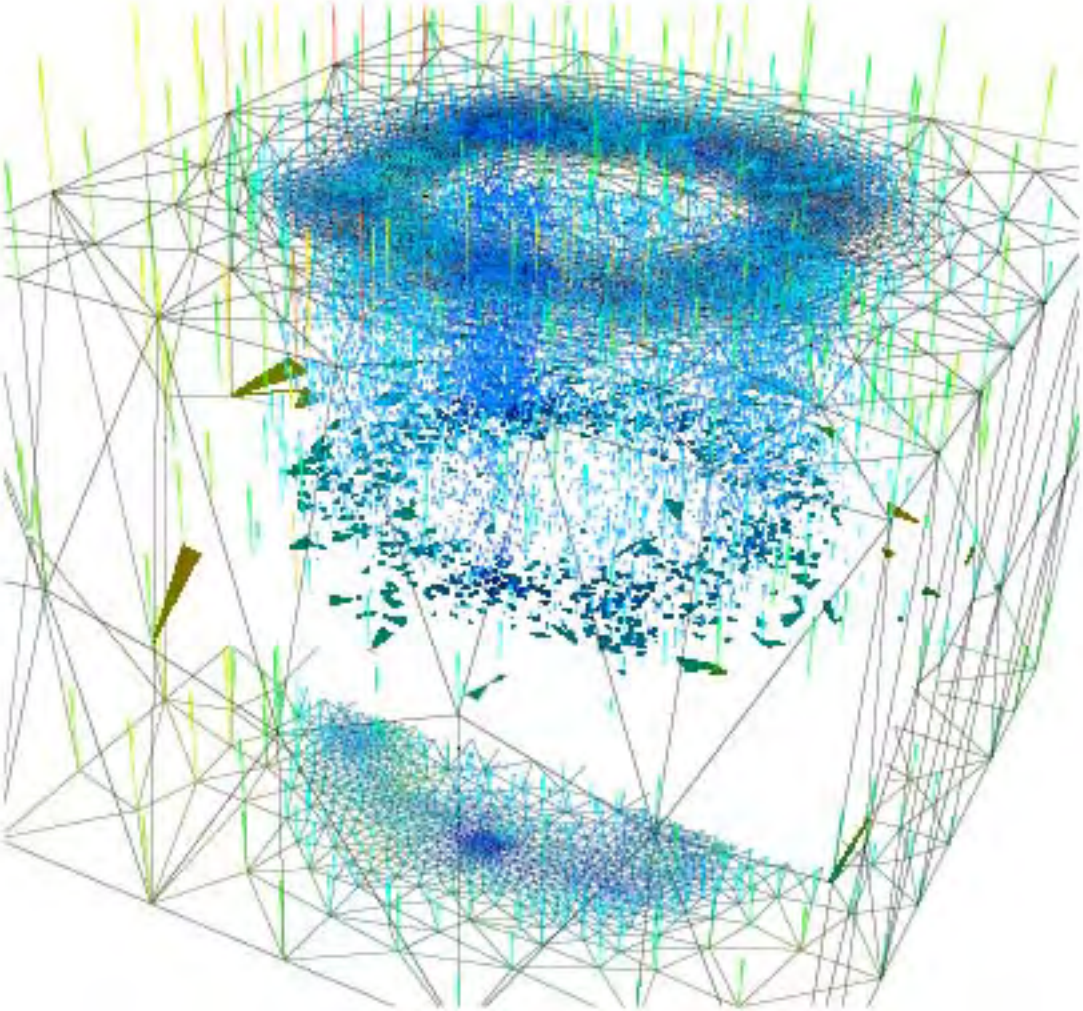

The metric tensor in form of a positive definite matrix defines anisotropically the desired mesh edge lengths at each node.

The desired edge length, h_i, in the direction of the i^{th} eigenvector, i.e, of the symmetric metric tensor M is defined as,

$$h_i = \frac{1}{\sqrt{\Lambda_i}}$$

where Λ_i is the eigenvalue associated with $\mathbf{e}_i$.

During mesh optimization the metric tensor is used to calculate distances via,

$$\|\mathbf{v}\| = \mathbf{v}^T M_v \mathbf{v},$$

where M_v is the average metric tensor along vector $\mathbf{v}$.

To define mesh optimization an element functional is defined in terms of the metric tensor and of properties a "good" mesh should exhibit for modeling.

Trials are therefore performed on local mesh connectivity and node position- in the case of a minimization problem defined- the aim being to find a local configuration that reduces functional value.

Defining the mesh functional as,

$$\mathcal{F} = \|\mathbf{F}\|_\infty,$$

where $\mathbf{F}$ is vector of element functionals for whole mesh and process terminates when $\mathcal{F}$ falls below some tolerance. There are many choices for the definition of the local functional $\mathcal{F}$ (see Venditti and Darmofal 2000, Kanupp, 2000).

Here we use geometrically based

$$\mathbf{F}_e = \frac{1}{2} \sum_{l \in L_e} (r_l - 1)^2 + \mu (\frac{\alpha}{\rho_e} - 1)^2.$$

where r_l is length w.r.t. edge centered metric tensor M_e of edge, L_e is set of edges of element e.

ρ_e is the radius of with respect to element centered, M_e of inscribed sphere of element e.

α is the radius of inscribed sphere of ideal equilateral element.

μ- controls trade off between size and shape.

Use of goal- oriented methods for efficient model reduction

Model reduction is powerful tool allowing systematic generation of cost-efficient representations of large-scale systems.

The problem of determining a reduced- model can best in a model- constrained optimization context (Willcox et al. 2005, Meyer and Matthias 2003).

In the goal- oriented formulation the reduced- model is chosen to optimally represent a particular output functional.

POD (proper orthogonal decomposition): *brief description*

POD is applied efficiently to reduce large- scale systems using the method of snapshots (Sirovich 1987).

The collection of snapshots

$$u^k(t_j), j = 1, \cdots, T, k = 1, \cdots, s,\ u^k(t_j) \in \mathcal{R}^n,$$

is a solution of governing equations at time t_j for parameter instance k. T time instants are considered yielding a total of S_T snapshots.

A snapshots matrix $U \in \mathbf{R}^{v \times S_T}$ is

$$U = [u^1(t_1), \cdots, u^4(t_T), u^2(t_I), \cdots, u^J(t_T)]$$

we refer to the $i-th$ column of U as the $i-$th snapshot U_i . POD basis vectors are chosen to be orthonormal set that maximizes the following cost,(Berkooz et al (1993)),

$$\Psi = arg\ max_{\phi} \frac{< |u, \phi|^2 >}{(\phi, \phi)} \qquad (*)$$

where (u, ϕ) is scalar product of basis vector with field $u(t)$ evaluated over the domain and $<>$ represents time- averaging operation.

$(*)$ is maximized when the n basis vectors are chosen to be the first n left singular vectors of U.

For fixed basis size the POD basis minimizes error between original snapshots and their representation in the reduced space defined by,

$$\mathbf{F} = \sum_{k=1}^{s} \sum_{t=1}^{T} [u^k(t_j) - \tilde{u}^k(t_j)]^T [u^k(t_j) - \tilde{u}^k(t_j)],$$

where $\tilde{u}^k(t_j) = \phi \phi^T u^k(t_j)$.

The error is equal to sum of singular values corresponding to the singular

vectors excluded from the basis,

$$\mathbf{E} = \sum_{i=n+1}^{S_T} \sigma_i.$$

The goal- oriented methods focus on reduction of the error for a particular output functional- rather than for the general state vector.

Also error minimized by optimization approach will be connected to the reduced order model- whereas POD is based purely on the set of snapshots data.

Such an approach was presented for a general linear time- invariant (LTI) dynamical system (Willcox et al. 2005),

$$M\dot{u} + Ku = f,$$

$$g = Cu,$$

with $u(0) = u_0$, with $\dot{u}(t)$ is derivative of $u(t)$ w.r.t. time.

Vector $f(t) \in \mathcal{R}^n$ defines input to system and matrix C defines q outputs of interest contained in output vector $g(t)$.

Meyer and Matthies (2003) have used POD (K-L) basis for nonlinear random fatigue evaluation of a wind turbine.

Using POD with goal oriented methods (Dual- Weighted Residual) an a-posteriori error estimate was obtained for a particular target functional of the solution.

This estimate was used for adaptively resizing number of basis vectors of POD to satisfy given error tolerance.

Also it was used to form very efficient low- dimensional basis specifically tailored for target functional of interest.

The basis yielded a significantly better approximation of the functional than the usual POD basis.

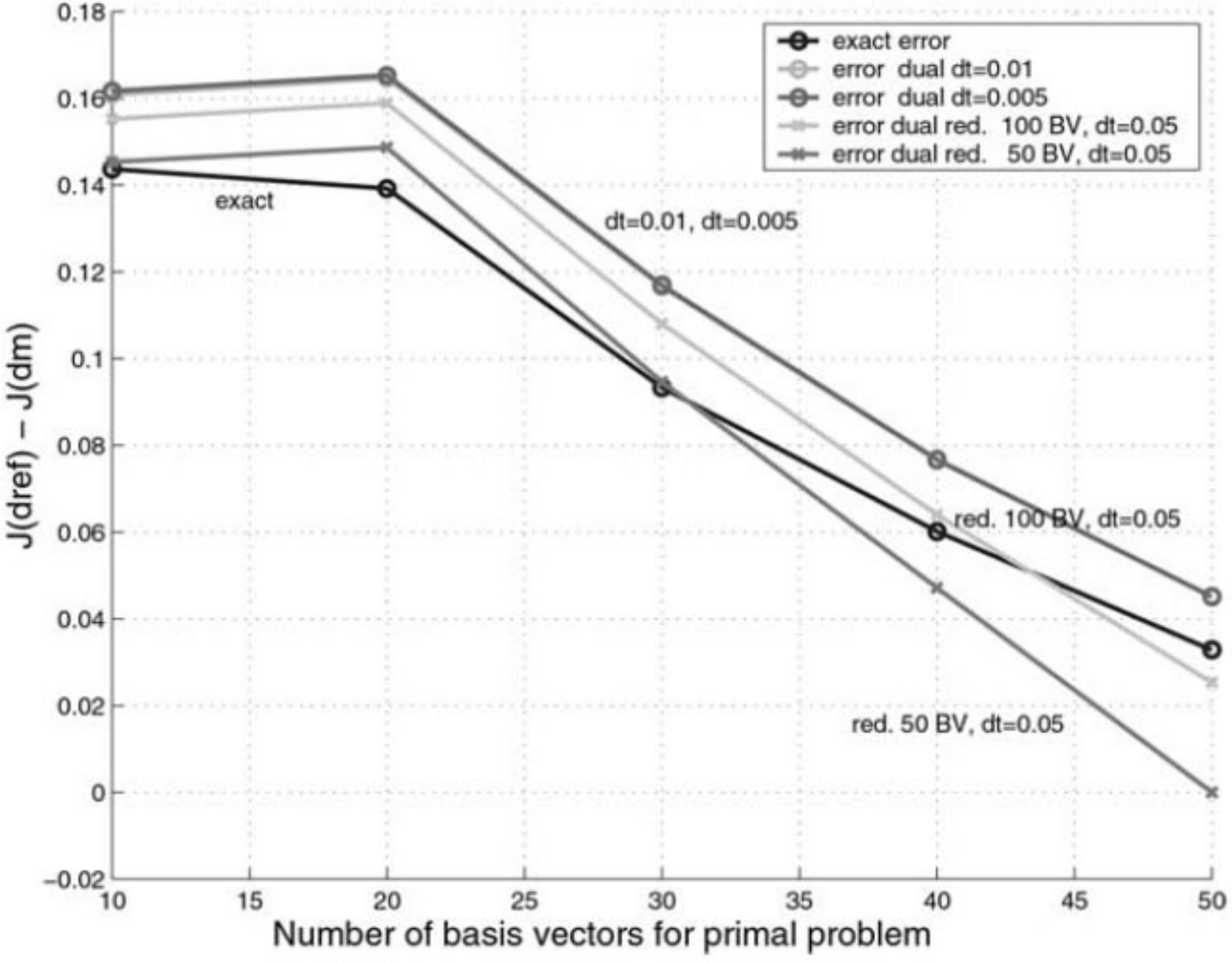

Fig. 8. Comparsion of exact and estimated error

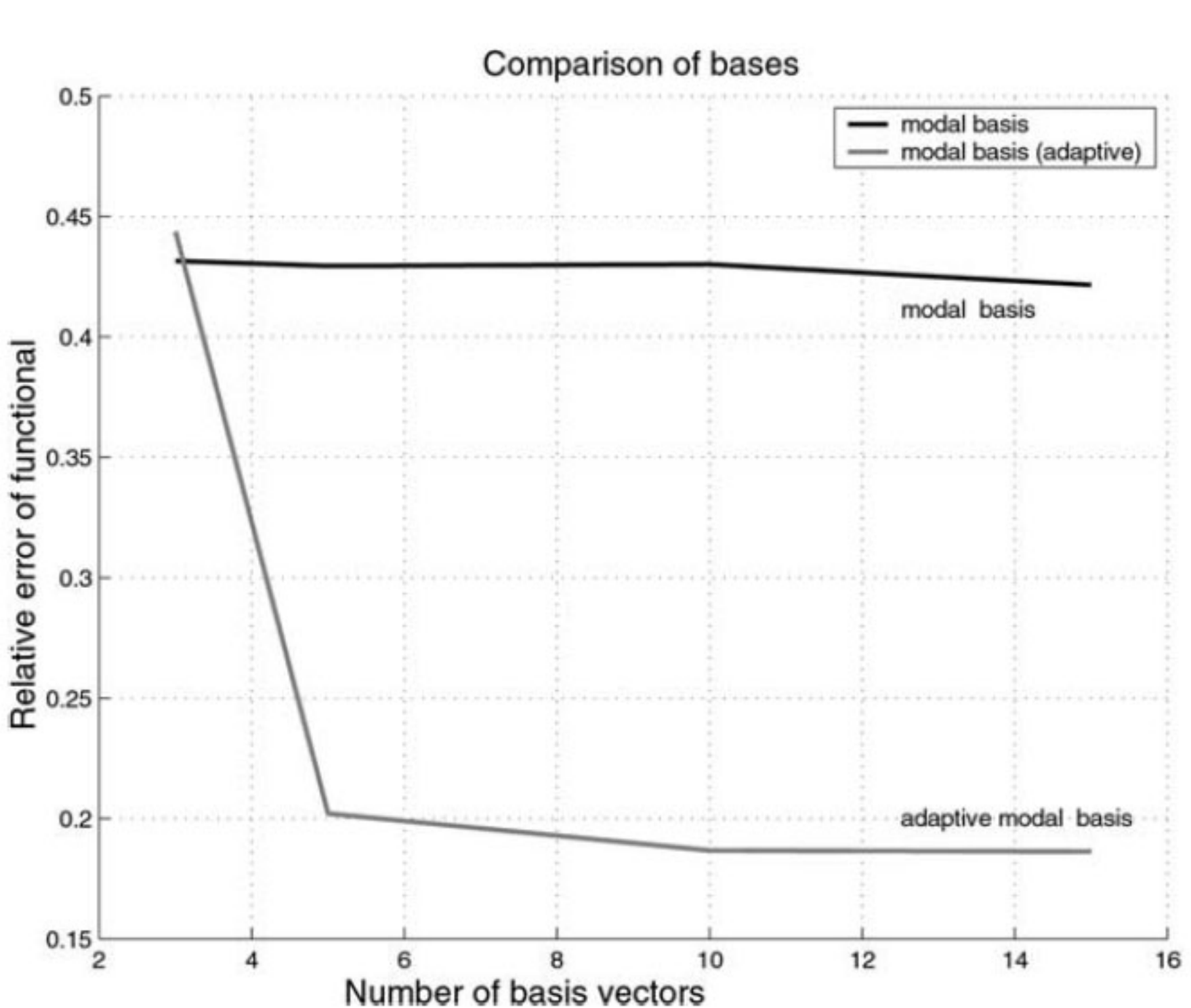

Fig. 10. Relative error of J over m for the modal basis

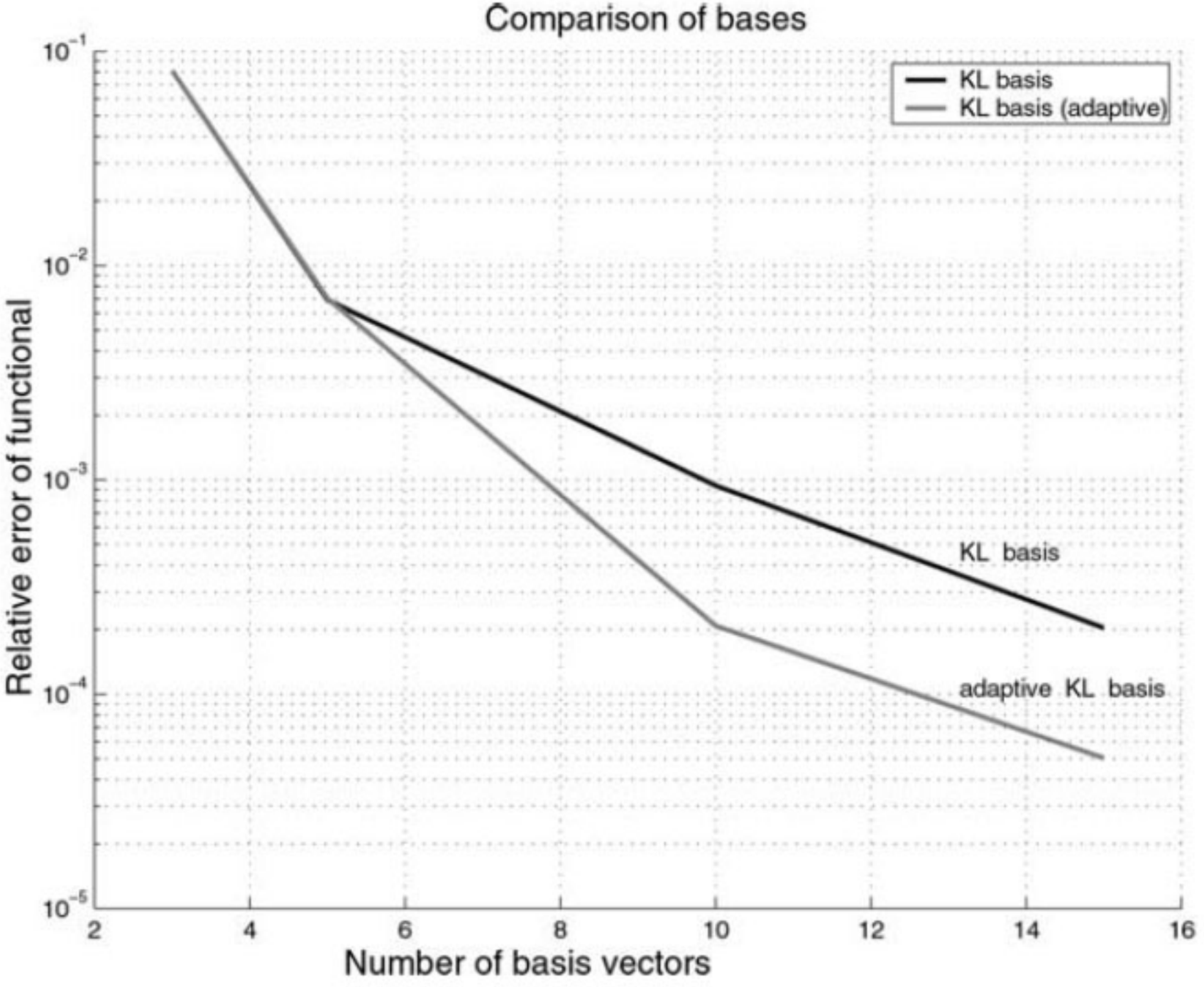

Fig. 11. Relative error of J over m for the KL basis

Summary and future work

- Future work on application of goal- based error measures for adaptive refinement.
- Introduce second order error information obtained from either second order adjoint model or leading Hessian singular vectors in energy norm to reflect integral outputs for dynamics or domain areas of interest.
- Use mesh adaptivity in data assimilation, i.e, construct approximate adjoint models and increase ability to adapt mesh to optimize accuracy of inverse problem.
- Provide improved targeted adaptive observations to optimize forecast accuracy (using SVD or adjoint sensitivity analysis).
- Develop ability to recognize suitable functionals reflecting dynamics of ocean flow for use in goal oriented adjoint correction methods